Journal of Medicinal Chemistry

Article

1,3-Dipolar cycloaddition, HPLC enantioseparation and docking studies of saccharin/isoxazole and saccharin/isoxazoline derivatives as selective carbonic anhydrase IX and XII inhibitors

Melissa D'Ascenzio, Daniela Secci, Simone Carradori, Susi Zara, Paolo Guglielmi, Roberto Cirilli, Marco Pierini, Giulio Poli, Tiziano Tuccinardi, Andrea Angeli, and Claudiu Trandafir Supuran

J. Med. Chem., **Just Accepted Manuscript** • DOI: 10.1021/acs.jmedchem.9b01434 • Publication Date (Web): 23 Jan 2020

Just Accepted

is published by the American Chemical Society. 1155 Sixteenth Street N.W., Washington, DC 20036

1,3-Dipolar cycloaddition, HPLC enantioseparation and docking studies of saccharin/isoxazole and saccharin/isoxazoline derivatives as selective carbonic anhydrase IX and XII inhibitors

Melissa D'Ascenzio[a§], Daniela Secci[a,*], Simone Carradori[b], Susi Zara[b], Paolo Guglielmi[a], Roberto Cirilli[c], Marco Pierini[a], Giulio Poli[d], Tiziano Tuccinardi[d], Andrea Angeli[e,f], Claudiu T. Supuran[e]

[a]*Dipartimento di Chimica e Tecnologie del Farmaco, Sapienza University of Rome, P.le A. Moro 5, 00185 Rome, Italy*

[b]*Department of Pharmacy, "G. d'Annunzio" University of Chieti-Pescara, Via dei Vestini 31, 66100 Chieti, Italy*

[c]*Centro nazionale per il controllo e la valutazione dei farmaci, Istituto Superiore di Sanità, Viale Regina Elena 299, 00161 Rome, Italy*

[d]*Department of Pharmacy, University of Pisa, Via Bonanno 6, 56126 Pisa, Italy*

[e]*Neurofarba Department, Section of Pharmaceutical and Nutraceutical Sciences, University of Florence, Via U. Schiff 6, 50019 Sesto Fiorentino (Florence), Italy*

[f]*Centre of Advanced Research in Bionanoconjugates and Biopolymers Department, "Petru Poni" Institute of Macromolecular Chemistry, 41A Grigore Ghica-Voda Alley, 700487 Iasi, Romania*

*Corresponding author: Daniela Secci, Dipartimento di Chimica e Tecnologie del Farmaco, Sapienza University of Rome, P.le A. Moro 5, 00185 Rome, Italy. E-mail: daniela.secci@uniroma1.it

[§]Current affiliation: D'Arcy Thompson Unit, School of Life Sciences, University of Dundee, Dundee (Scotland). E-mail: m.dascenzio@dundee.ac.uk

Abstract

Two series of saccharin/isoxazole and saccharin/isoxazoline hybrids were synthesised by 1,3-dipolar cycloaddition. The new compounds showed to be endowed with potent and selective inhibitory activity against the cancer-related human carbonic anhydrase (hCA) IX and XII isoforms in the nanomolar range, while no affinity was encountered for off-targets such as hCA I and II. Successive enantioseparation on a mg-scale of the most representative compounds led to the discovery that (*S*)-isomers were more potent than their corresponding (*R*)-enantiomers. Lastly, molecular modelling studies were conducted in order to define those structural requirements that were responsible for the discrimination among selected human isoforms of carbonic anhydrases. Two nanomolar hCA IX and XII inhibitors were also screened for their selective toxicity against non tumoral primary cells (fibroblasts) and against a breast adenocarcinoma cell line (MCF7) in hypoxic environment. The efficacious combination of these compounds with doxorubicin on MCF7 cells was demonstrated after 72 h of treatment.

Keywords: Saccharin, isoxazole, isoxazoline, chiral HPLC, docking, carbonic anhydrase inhibitors.

Introduction

Carbonic anhydrases (CAs, EC 4.2.1.1) are ubiquitous metalloenzymes that catalyse the interconversion of carbon dioxide and water into bicarbonate and hydrogen ions.[1] Among the seven CA families, αCA are further categorized in 15 diverse human (h) isoforms playing pivotal roles in a multitude of physiological functions and pathological conditions.[2] hCA I and II are cytosolic proteins with high enzymatic efficiency that are constitutively expressed in all tissues. Conversely, hCA IX and XII are membrane-associated proteins that can be overexpressed in the hypoxic tumour environment, with CA IX not significantly present in the majority of healthy tissues.[3] Owing to the peculiar role of these multidomain enzymes in many solid tumours, compounds that are able to act against the extracellular facing carbonic anhydrases IX and XII are currently under investigation.[4,5]

In fact, recent research efforts have led to the identification of a large plethora of CAs inhibitors characterized (or not) by a zinc binding group, as the presence of a metal ion in the active site constitutes one of the most conserved features within this family of enzymes.[6-11]

In particular, saccharin derivatives have been reported as good hCAs inhibitors by various research groups that, in the last few years, focused their attention toward the development of new derivatives based on this scaffold.[12-17] Analysing the structure and substitution pattern of previously published inhibitors possessing a saccharin core, it was highlighted that two general approaches had been exploited for the design of new compounds (**Figure 1**): the first strategy relied on the substitution of the benzene ring of saccharin while maintaining the cyclic secondary sulfonamide functional group in its unsubstituted form (**Figure 1**, **I** and **II**). This approach produced inhibitors endowed with activity in the nanomolar range against isoforms IX and XII, although residual activity against the off-targets hCA I and hCA II was unfortunately retained.[15,18]

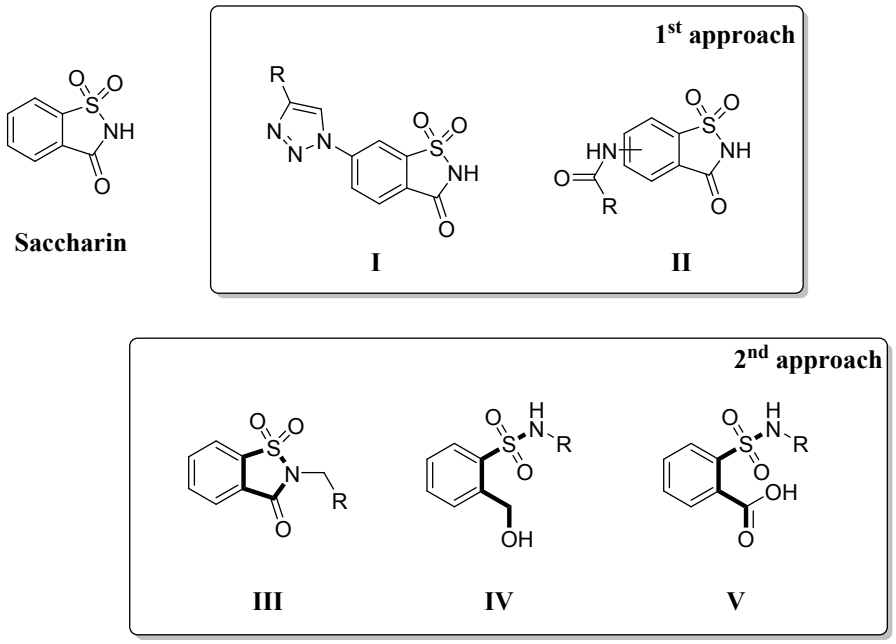

Figure 1. The two different approaches used for the synthesis of saccharin-based hCAs inhibitors.

The second approach was based on the substitution of the cyclic secondary sulfonamide with different groups in order to obtain *N*-substituted saccharins (**Figure 1**, **III**). These molecules were

effective inhibitors of hCA IX and XII, even if a few of them retained activity against off-target isoforms.[14,17] Successive efforts focused on obtaining the "open" form of these compounds using two synthetic strategies: the reductive opening of the heterocyclic ring to give a secondary sulfonamide and benzylic alcohol (**Figure 1**, **IV**),[13] or the hydrolysis of the cyclic sulfonamide under basic conditions to generate a carboxylic acid and a secondary sulfonamide (**Figure 1**, **V**).[19] Our research group contributed mostly to the development of *N*-substituted saccharins, which meant that a compound obtained by 1,3-dipolar cycloaddition between *N*-propargyl substituted saccharin and *N*-hydroxy-4-nitrobenzimidoyl chloride was already reported in one of our first works,[13,14,17] among others (**Figure 2**).

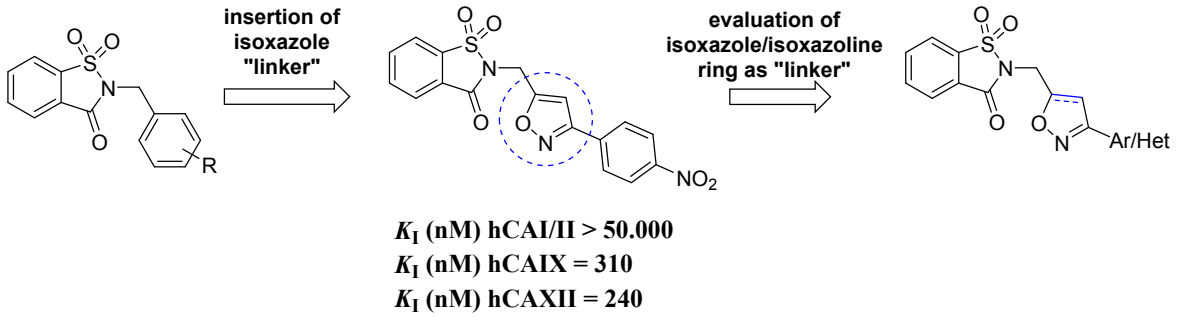

Figure 2. Design of new saccharin/isoxazoline and saccharin/isoxazole derivatives.

The first compound endowed with a heterocyclic "linker" between the methylene and the phenyl ring showed activity in the nanomolar range only against tumor-related isoforms, while being ineffective against the two main off-targets. In light of the above, we designed two series of new inhibitors obtained by inserting two different heterocyclic systems as linker groups: the isoxazole and isoxazoline ring, respectively. The chosen linkers possess some common characteristics, e.g. they are both five-membered rings containing nitrogen and oxygen, they display identical connectivity and position of substituents. However, the isoxazole ring is a flat-aromatic system that can give π-stacking interactions inside the active site; on the other hand, isoxazoline - the 4,5-dihydrogenated form of isoxazole – is not aromatic and possesses two tetrahedral carbon atoms that

alter the flat conformation (although π-interactions could still be established using the double bond in the ring). Furthermore, the presence of four different substituents on one of the two tetrahedral carbon (C5 of isoxazoline) accounts for the existence of a stereogenic center. Therefore, all the saccharin/isoxazoline compounds can exist as a pair of enantiomers that can be resolved and tested in order to determine the configuration preferred by the enzymes and, in conclusion, the eutomer.

The inhibition data obtained from the biological assays were further corroborated through molecular modelling studies including docking and molecular dynamics (MD) simulations. In particular, we focused our attention on the most interesting compounds in order to determine the interactions established inside the active site of hCAs that could help rationalise activity and selectivity. Two potent hCA IX and XII inhibitors were selected to further assess their effects on viability and cytotoxicity in an *in vitro* model of normal human primary cells (fibroblasts), and, at the same time, the antiproliferative effect of hCA IX and XII inhibitors in combination with doxorubicin, on an adenocarcinoma breast cancer cell line (MCF7 cells).

Chemistry

The synthesis of this small library of new saccharin derivatives followed a multi-step approach,[20,21] which led to the preparation of the appropriate reagents for the final 1,3-dipolar cycloaddition, *i.e.* allyl/propargyl *N*-substituted saccharins (**S1-S2**) and hydroxyiminoyl acid chlorides (chloro-oximes **C1-C9**). Final compounds (**1a-9a** and **1b-9b**) were obtained in moderate yields (**Scheme 1**).

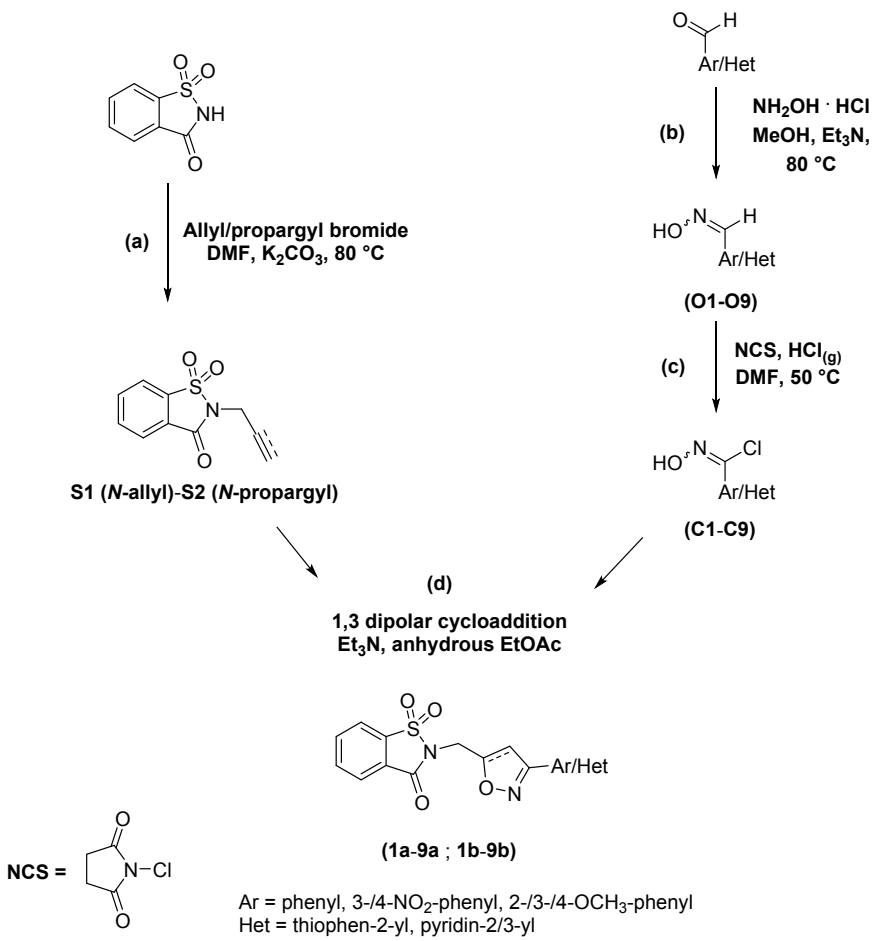

Scheme 1. Synthetic approach for the synthesis of new derivatives **1a-9a** and **1b-9b**.

N-alkylated saccharins (**S1-S2**) were obtained following our previously reported procedure,[17] which involved a nucleophilic substitution reaction between saccharin and allyl/propargyl bromide (**Scheme 1**, **a**). The hydroximinoyl acid chlorides (chloro-oximes) were synthesised in two steps from the corresponding benzaldehydes.[22] The first step (**Scheme 1**, **b**) required the reaction between the appropriate aldehyde with hydroxylamine hydrochloride in the presence of triethylamine in methanol (80 °C) to give the corresponding oximes (**O1-O9**). At a later time, the freshly synthesised oximes (**O1-O9**) were reacted with *N*-chlorosuccinimide (NCS) in *N*,*N*-dimethylformamide (DMF) in the presence of catalytic amounts of gaseous hydrogen chloride ($HCl_{(g)}$) (**Scheme 1**, **c**). In fact, Howe *et al.* observed that the reaction of NCS with benzaldoximes exhibited an induction period that could be reduced through the addition of small amounts of gaseous HCl. In this way, we avoided the fairly exothermic behaviour observed when the reaction

initiates after a considerable portion of NCS has been added.[22] The resulting chloro-oximes were not contaminated by side-products (*i.e.* chlorinated ring products) and could be used without purification in the next 1,3-dipolar cycloaddition step. In this reaction, the 1,3-dipole was generated *in situ* by dehydrohalogenation of the corresponding chloro-oxime (**C1-C9**) and then reacted with the dipolarophile (*N*-allyl/propargyl saccharins) in dry ethyl acetate (**Scheme 1**, **d**). The regioselectivity of the isoxazoline ring formation is usually controlled by the energy of the interacting orbitals (frontier molecular orbitals, FMO), although in some cases the electronically preferred orientation might be disfavoured due to steric effects.[23] However, the reaction of nitrile oxides with monosubstituted olefins is quite exclusive, giving only (or predominantly) 5-substituted isoxazolines, regardless of the nature of the substituent on the dipolarophile. Similarly, the cycloaddition of nitrile oxides to acetylenic dipolarophiles leads to 5-substituted isoxazoles.[21,23]

The purity of all final compounds was >95% as determined by HPLC analysis, employing two different chromatographic methods for isoxazoline and isoxazole derivatives. The compounds were analysed using gradient elution with a binary mobile phase composed by water and acetonitrile, and were shown to be ≥95% HPLC pure (Figures S4-S10; S15-S23). The compounds **8a** and **9a** were evaluated for their purity after chiral resolution through the analytical checks of the enantiomeric purity of each enantiomer (Figures S11-S14).

Two-dimensional (2D) Nuclear Overhauser Enhancement Spectroscopy (NOESY) NMR

The regioselectivity of the cycloaddition step was studied using compound **3b** as a model. Compound **3b** was synthesised by the reaction of *N*-hydroxy-pyridine-2-carbimidoyl chloride and *N*-propargyl saccharin. 2D-NMR (NOESY) analysis conducted on compound **3b** demonstrated a spatial relationship between proximal protons that could be highlighted in 5-substituted isoxazoles (**Figure 3**, **a**) but not in their 4-substituted analogues (**Figure 3**, **b**), thus confirming the overall tendency of this type of 1,3-dipolar cycloadditions to produce 5-substituted rings.

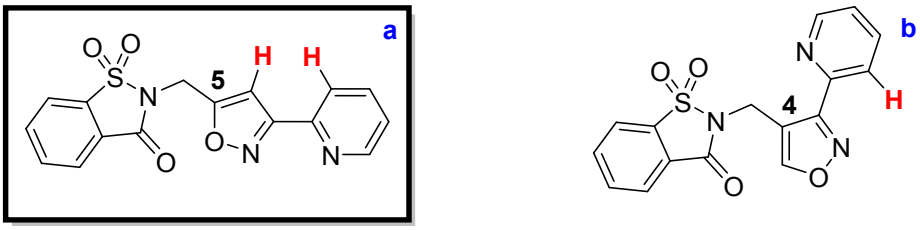

Figure 3. Structural isomers originated by the 1,3-dipolar cycloaddition of *N*-hydroxy-pyridine-2-carbimidoyl chloride and *N*-propargyl saccharin: (**a**) compound **3b**; (**b**) alternative structure proposed for compound **3b**.

Chiral resolution of compounds 8a and 9a

The reaction between *N*-allyl saccharin and chloro-oximes **C1-C9** determined the generation of a chiral centre (carbon C5) on the isoxazoline ring. In an attempt to determine whether hCA isoforms would show any preference for one enantiomer over the other, compounds **8a** and **9a** were submitted to enantioselective HPLC separation. Pure enantiomers of each compound were obtained in mg-amount and submitted for further assays (**Figure 4**).

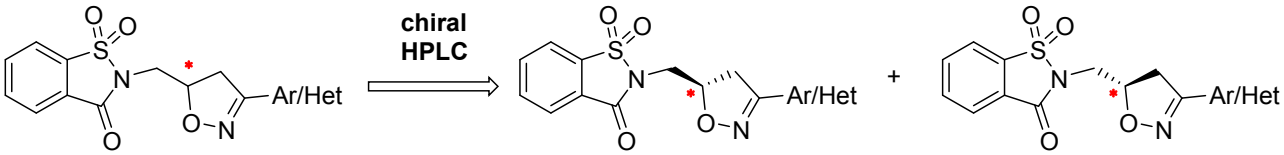

Figure 4. Resolution of saccharin/isoxazoline compounds by chiral HPLC.

All the synthesized saccharin/isoxazoline and saccharin/isoxazole derivatives were then tested to evaluate their inhibitory activity against the ubiquitous off-target isoforms, hCA I and II, as well as the cancer-related ones, hCA IX and XII, using a stopped-flow CO_2 hydrase assay method.[24] The hCAs inhibition data (K_I) are summarized in **Table 1**. K_i ratios between target and off-target isoforms were also reported in square brackets as a measure of compound selectivity. The hCA

tested in this work were in line with those reported in previous works, for better comparison and to improve the SAR within the saccharin-based scaffold.

Results and discussion

Two-dimensional Nuclear Overhauser Enhancement NMR

The interaction between the two protons highlighted in red in **Figure 3** was highlighted in the NMR-NOESY spectrum reported in **Figure 5** below.

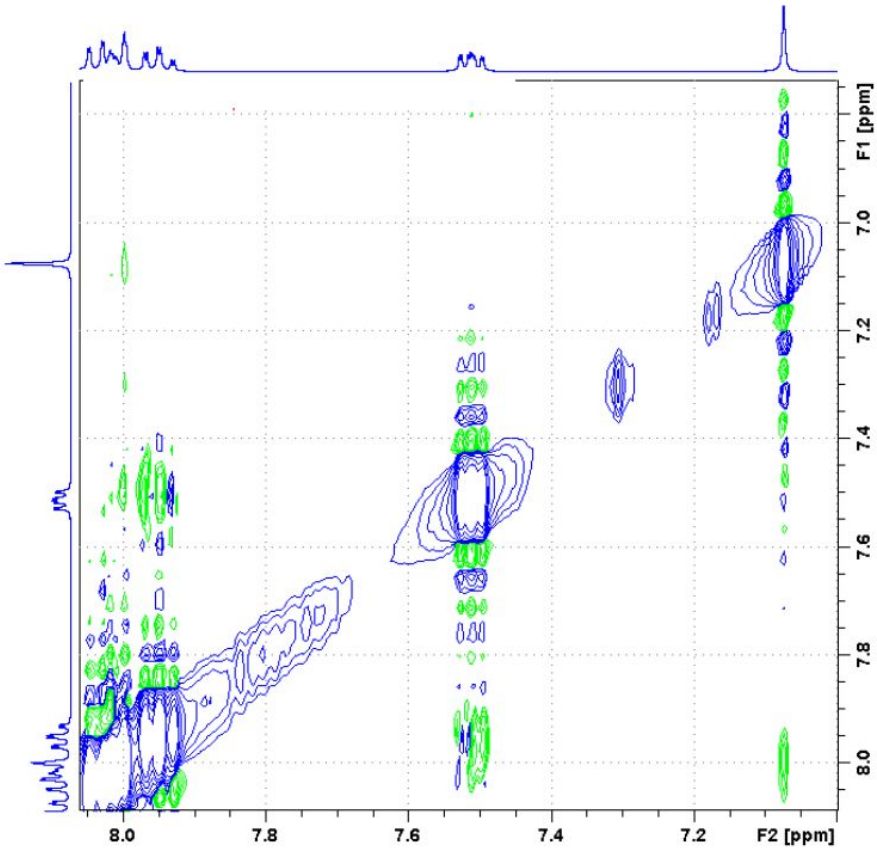

Figure 5. NMR-NOESY of compound **3b**.

The interaction between protons with spatial proximity was confirmed by the presence of the "green" circles along the ideal line that connects proton C4(H) of the isoxazole ring (singlet at ~7.06 ppm) and the pyridine signals between 7.90 and 8.10 ppm, which contain the proton at the C3 position of the pyridine ring. This outcome confirmed the regioselectivity of the reactions in our experimental conditions.

Chiral resolution of compounds 8a and 9a

The semipreparative enantioseparation of **8a** and **9a** was carried out on coated amylose-based Chiralpak AS-H chiral stationary phase using pure ethanol as a mobile phase. In **Figure 6** we reported the mg-scale enantioseparation and analytical checks of the enantiomeric purity of the collected enantiomers. Both enantiomeric separations gave yields of about 85% and enantiomeric excess of >98% for both enantiomers (S11-S14).

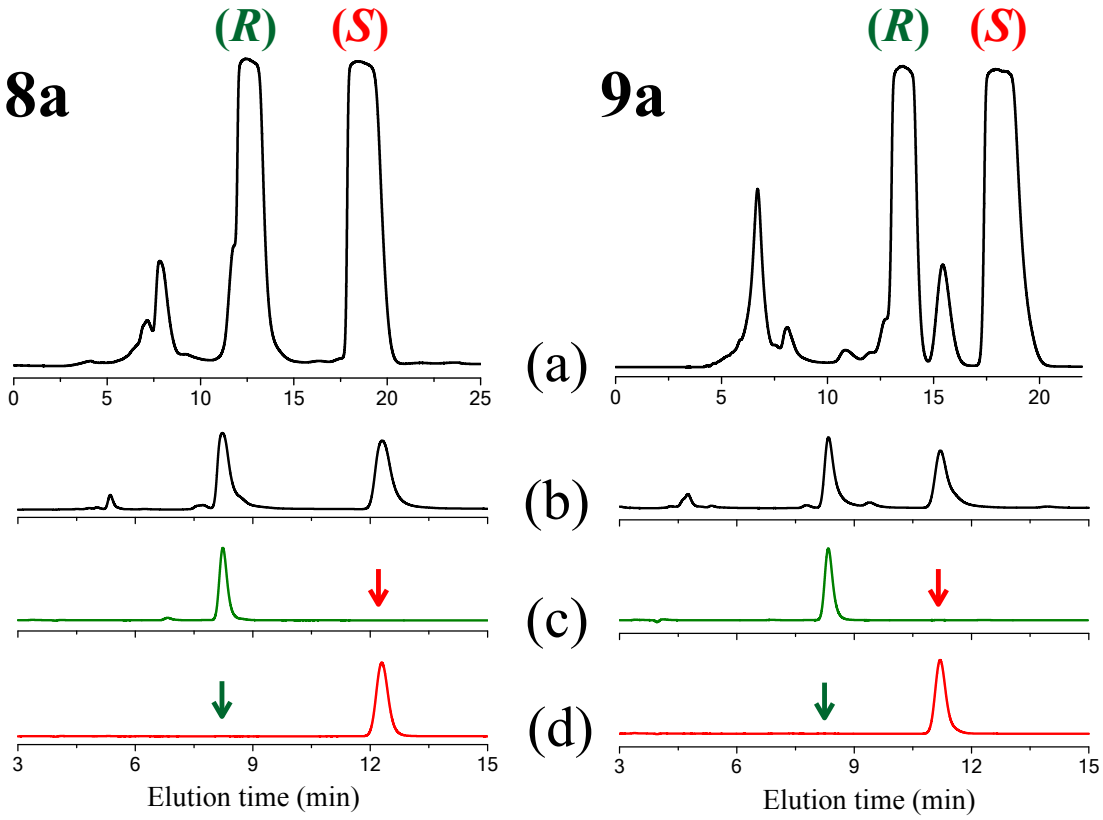

Figure 6. Traces (**a**): typical chromatogram illustrating the semipreparative enantioseparation of 3 mg of **8a** and 2 mg of **9a** on a 250 x 10 mm i.d. AS-H column. Mobile phase: ethanol; flow rate: 2.5 mL/min; temperature: 40 °C; detector: UV at 280 nm. Traces (**b**): analytical resolution of **8a** and **9a**. Traces (**c**) and (**d**): purity check of the enantiomers collected at a semipreparative scale. Mobile phase: ethanol; flow rate: 0.8 mL/min; temperature: 40 °C; detector: UV at 254 nm.

Assignment of the absolute configuration to compounds 8a and 9a

The absolute configuration of both enantiomers of **8a** and **9a** was determined by comparison of the experimental and computed electronic circular dichroism (ECD) spectra (**Figure 7**). A detailed description of the adopted procedure is provided in the Experimental Section. In brief, the obtained spectra allowed us to assign the (*S*)-configuration to the more retained species and the (*R*)-configuration to the first eluted enantiomers, as shown in **Figure 7** for both compounds **8a** and **9a**.

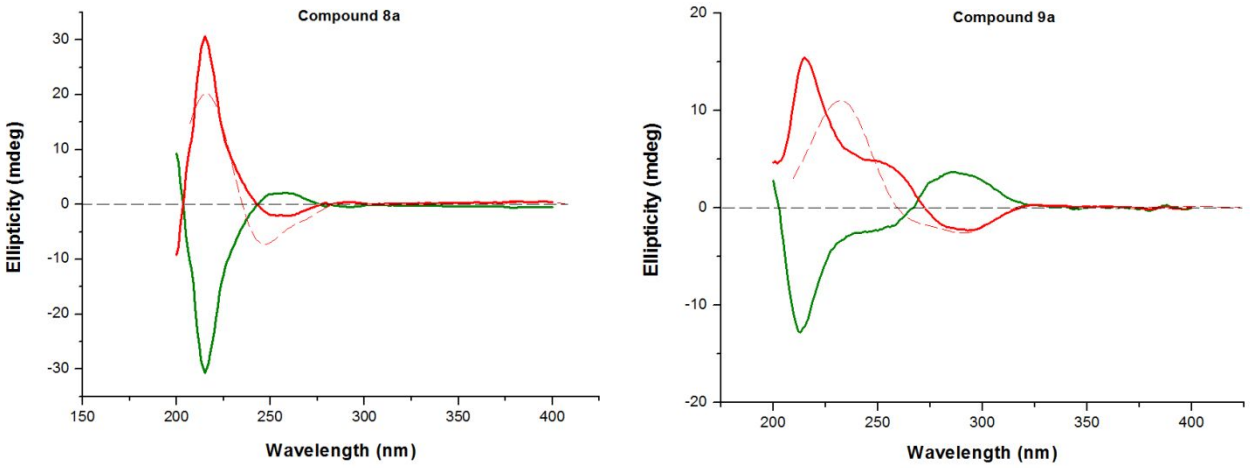

Figure 7. Experimental (full line) and calculated (dashed line) ECD spectra of the enantiomers of **8a** (left side) and **9a** (right side) in ethanol. In both graphs the first enantiomer eluted from the chiral HPLC column is shown as a green line, while the second one is shown as a red line. The red dashed traces refer to the ECD spectra calculated for the enantiomer (*S*)-**8a** and (*S*)-**9a**, respectively.

Inhibition of hCA I, II, IX, and XII

Comparing the activity of compounds **1a-9a** and **1b-9b** with the *N*-allyl/propargyl saccharin parent drugs (**S1** and **S2**), it was possible to assess that the insertion of an isoxazoline/isoxazole ring bearing aromatic or heteroaromatic substituents improved both activity and isoform selectivity. In particular, the effects of these changes were more pronounced with regards to selectivity. As a matter of fact, data reported in **Table 1** showed that, except for derivatives (*R*)-**9a** and (*S*)-**9a**, all the synthesised compounds were selective inhibitors of hCA IX and hCA XII. Moreover, a preferential

affinity for isoform XII was observed, with K_I spanning from 1.0 nM ((*S*)-**9a**) to 240 nM (derivative **2b**). The nature of the linker (isoxazoline rather than isoxazole) or the substituents on the phenyl ring, as well as the heterocyclic system, influenced the inhibitory activity against the tested isoforms. Due to the relatively small size of the two series, it was difficult to establish a clear structure-activity trend. However, a few interesting observations could be made: compounds **1a** and **1b**, characterised by the presence of a NO_2 group on the *meta* position of the phenyl substituent, showed similar inhibitory activity against isoform XII (**1a**, K_I hCA XII = 76.5 nM; **1b**, K_I hCA XII = 57.3 nM), while compound **1a** was more effective than **1b** against isoform IX (**1a**, K_I hCA IX = 102.9 nM; **1b**, K_I hCA IX = 230.2 nM). Compounds **2a** and **2b**, both possessing a *p*-NO_2 substituted phenyl ring, displayed a similar trend in hCA IX inhibition, while compound **2b** (containing the isoxazole linker) showed impaired activity against isoform XII (**2a**, K_I hCA XII = 77 nM; **2b**, K_I hCA XII = 240 nM). In the case of these four derivatives (**1a-2a**, **1b-2b**) it could be noted that starting from **1a**, containing a *m*-NO_2 substituted phenyl ring bound to the isoxazoline ring, to compound **2b** endowed with *p*-NO_2 substituted phenyl ring connected to the isoxazole system, there was a decrease of activity against hCA IX (**Table 1**). This trend was opposite compared to derivatives spanning from **6a** to **7b**, which were characterised by the presence of a methoxy substituent (OMe). Indeed, compound **7b** - endowed with an isoxazole linker and *p*-OMe substituted phenyl ring - showed good inhibitory activity against isoform IX (K_I hCA IX = 22.1 nM). All the other derivatives possessing a methoxy group were found to be inactive (**5a**, **5b**, **6a**), or at least less effective (**6b** and **7a**) against isoform IX, when compared to compound **7b**. On the other side, they were good inhibitors of hCA XII ($7.0 \leq K_I$ hCA XII (nM) ≤ 9.4), with the best inhibitory activity exhibited by compound **6b**. These data seemed to suggest that the nature of the linker did not favour one isoform over the other and did not affect enzyme inhibition in a specific manner. In fact, the transition from an isoxazoline ring in **1a** to the isoxazole ring of **1b** increased the activity against hCA XII, while reduced the inhibitory effect against hCA IX. In the case of compounds **2a-2b**, we observed a reduction of activity against both tumour-related isoforms when

passing from the isoxazoline linker (**2a**) to an isoxazole ring (**2b**). The change of linker type for pairs **6a-6b** and **7a-7b** only influenced the inhibitory activity against hCA IX, while hCA XII was not affected, showing almost comparable inhibition data. Albeit further substitution patterns still need to be evaluated, these preliminary results showed that the nature of the heteroaromatic linker, together with the type and position of aromatic substituent, could have a synergistic effect on the inhibitory activity of the corresponding derivatives, rather than being independent features.

Bioisosteric heterocyclic systems bound to the linker moiety were also evaluated. For example, compounds **3a** and **3b** were endowed with a pyridin-2-yl moiety. These derivatives showed similar activity against hCA IX (**3a**, K_I hCA IX = 258.2 nM; **3b**, K_I hCA IX = 245.4 nM), whereas compound **3a** exhibited better activity against hCA XII compared to its isoxazole containing analogue (**3a**, K_I hCA XII = 9.7 nM; **3b**, K_I hCA XII = 66.5 nM). Derivatives **4a** and **4b**, which were characterised by the presence of a pyridin-3-yl system, showed comparable activity against isoform XII, while they differed for activity on hCA IX (**4a**, K_I hCA IX = 273.5 nM; **4b**, K_I hCA IX = 86.2 nM). These data suggested that the influence of the linker is not unequivocal. Compounds containing phenyl (**8b**) or thiophene (**9b**) substituents bound to the isoxazole ring showed low nanomolar inhibition of hCA XII (**8b**, K_I hCA XII = 7.5 nM; **9b** K_I hCA XII = 8.2 nM), while derivative **9b** displayed better affinity than **8b** with regards to hCA IX (**8b**, K_I hCA IX = 50.9 nM; **9b**, K_I hCA IX = 7.5 nM). Therefore, the five-membered heterocyclic system seemed to be the best tolerated group bound to the linker. Finally, the evaluation of potential chiral recognition operated by specific hCAs isoforms was evaluated by subjecting previously purified enantiomers of compounds **8a** and **9a** to biological testing. The enantiomers of compound **8a** were ineffective towards off-targets hCA I and hCA II, while their inhibitory activity against hCA IX and XII was deemed to be comparable. Therefore, we could conclude that in this case the enzymes did not exhibit a "chiral preference" between the two enantiomers (**Table 1**). A different outcome was obtained for the enantiomers of compound **9a**. The (*S*)-enantiomer of derivative **9a** lacked that selectivity for the tumour-related isoforms that was recorded when both enantiomers were tested as

a racemic mixture, as it inhibited both the off-targets hCA I and II (K_I hCA I = 365 nM; K_I hCA II = 13.1 nM). However, it also exhibited a very low nanomolar affinity for hCA XII (**(*S*)-9a**, K_I hCA XII = 1.0 nM) and hCA IX (**(*S*)-9a**, K_I hCA IX = 2.4 nM), resulting in the most potent inhibitor of the series. The (*R*)-enantiomer of compound **9a** was inactive against hCA II, showing poor residual activity towards isoform I (**(*R*)-9a**, K_I hCA I = 358.0 nM), while the activity against the two tumour related isoforms remained in the low nanomolar range (**(*R*)-9a**, K_I hCA IX = 26.4 nM; K_I hCA XII = 8.6 nM), although inferior to that of the (*S*) enantiomer. In the light of the above, we could conclude that due to the chiral properties of compound **(*S*)-9a**, this is the eutomer of the enantiomeric pair.

Table 1. Inhibition data of selected human CA isoforms (hCA I, II, IX and XII) with compounds **1a-9a** and **1b-9b** reported here and the standard sulfonamide inhibitor acetazolamide (AAZ) by a stopped flow CO_2 hydrase assay.

Compd	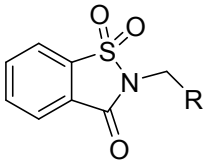	K_I (nM) [a]			
	R	hCA I [hCA I/hCA XII][b]	hCA II [hCA II/hCA XII][b]	hCA IX [hCA IX /hCA XII] [b]	hCA XII
S1[17]		>10000 [>106.4]	86 [0.9]	140 [1.5]	94
S2[17]		>10000 [>17.5]	58 [0.1]	210 [0.4]	570
1a	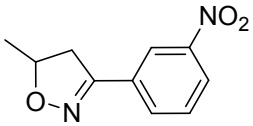	>10000 [>130.7]	>10000 [>130.7]	102.9 [1.3]	76.5
1b	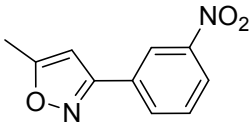	>10000 [>174.5]	>10000 [>174.5]	230.2 [4.0]	57.3
2a	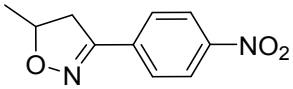	>10000 [>129.9]	>10000 [>129.9]	235.1 [3.1]	77.0
2b	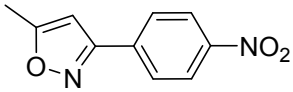	>10000 [>41.7]	>10000 [>41.7]	310 [1.3]	240
3a	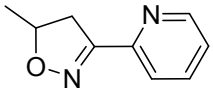	>10000 [>1030.9]	>10000 [>1030.9]	258.2 [26.6]	9.7

3b	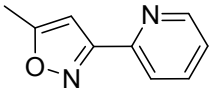	>10000 [>150.4]	>10000 [>150.4]	245.4 [3.7]	66.5
4a	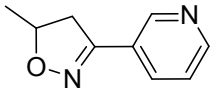	>10000 [>1087]	>10000 [>1087]	273.5 [29.7]	9.2
4b	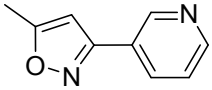	>10000 [>1250]	>10000 [>1250]	86.2 [10.8]	8.0
5a	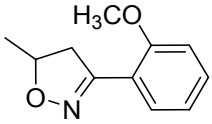	>10000 [>1063]	>10000 [>1063]	>10000 [>1063]	9.4
5b	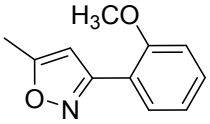	>10000 [>1075]	>10000 [>1075]	>10000 [>1075]	9.3
6a	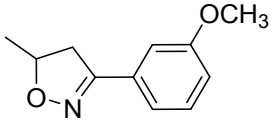	>10000 [>1315.8]	>10000 [>1315.8]	>10000 [>1315.8]	7.6
6b	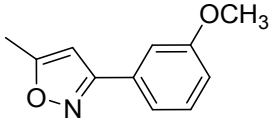	>10000 [>1428.6]	>10000 [>1428.6]	247.1 [35.3]	7.0
7a	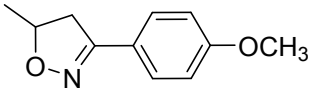	>10000 [>1234.6]	>10000 [>1234.6]	139.1 [17.2]	8.1
7b	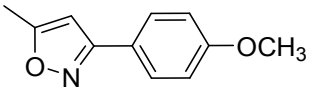	>10000 [>1250]	>10000 [>1250]	22.1 [2.8]	8.0
(*R*)-8a	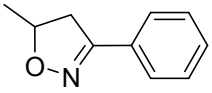	>10000 [>204.5]	>10000 [>204.5]	30.0 [0.6]	48.9
(*S*)-8a		>10000 [>274]	>10000 [>274]	29.3 [0.8]	36.5
8b	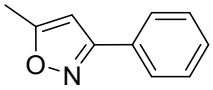	>10000 [>1333.3]	>10000 [>1333.3]	50.9 [6.8]	7.5
(*R*)-9a	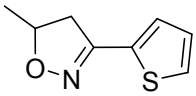	358 [41.6]	>10000 [>1162.8]	26.4 [3.1]	8.6
(*S*)-9a		365 [365]	13.1 [13.1]	2.4 [2.4]	1.0
9b	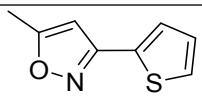	>10000 [>1219.5]	>10000 [>1219.5]	7.5 [0.9]	8.2
AAZ		250 [43.8]	12 [2.1]	25 [4.4]	5.7

[a]Mean from 3 different assay, by a stopped flow technique (errors were in the range of ± 5-10% of the reported values). [b]K_Is ratio for the indicated enzyme isoforms.

Molecular modelling studies

Molecular modelling studies, including docking and molecular dynamics simulations, were performed with the purpose of identifying a reliable binding mode into hCA XII and hCA IX for this novel series of saccharin ligands, in an attempt to rationalise their activity and selectivity profile (**Figure 8**). Compound **8b**, which showed to be one of the most potent and selective hCA XII and hCA IX inhibitor, was used as a reference compound of the series and docked into the X-ray structures of the two enzyme isoforms (PDB codes 1JD0 and 3IAI for hCA XII and hCA IX, respectively). The software GOLD with GoldScore fitness function was used for this study. The ligand-protein complexes predicted by docking were then refined and analysed through MD simulation studies. As shown in **Figure 8**, according to the binding mode predicted by the computational protocol, compound **8b** interacted with hCA XII by coordinating the prosthetic zinc ion in the active site of the enzyme with one of the two sulfonamide oxygen atoms belonging to the saccharin scaffold, while the other oxygen of the sulfonamide fragment forms an H-bond with the hydroxyl group of T227 that is maintained for most of the MD simulation. This latter oxygen shows an additional H-bond with the backbone oxygen of T227. A further H-bond is then observed between the carbonyl oxygen of the ligand and the amide group of Q117 side chain. The phenyl ring of the ligand saccharin core is placed in a mainly hydrophobic pocket constituted by W32, N92, H94, H121 and H119, forming a stable π-π stacking with the imidazole ring of this latter residue and lipophilic interactions with the other residues. Finally, the phenylisoxazole group of compound **8b** interacts with the residues belonging to the lipophilic side of the enzyme catalytic site, forming hydrophobic contacts with V147, S158, S161, L167, L225, and P229. The binding mode predicted for the ligand into hCA IX was similar to that generated for hCA XII. In fact, compound **8b** showed the same orientation into the hCA IX binding cavity, with the phenylisoxazole moiety laying on the hydrophobic wall of the catalytic site and the saccharin scaffold placed in proximity of the zinc ion, with the fused phenyl ring located into the small pocket

delimited by W141, N198, H200, Q203, H226 and H228. The ligand forms an H-bond with Q224 as observed in hCA XII (with the homologue residue Q117) through the carbonyl oxygen and coordinates the zinc ion with a sulfonamide oxygen. Moreover, the compound forms the two H-bonds with the backbone nitrogen of T333 (homologue of T227 in hCA XII) and the hydroxyl group of the same residue.

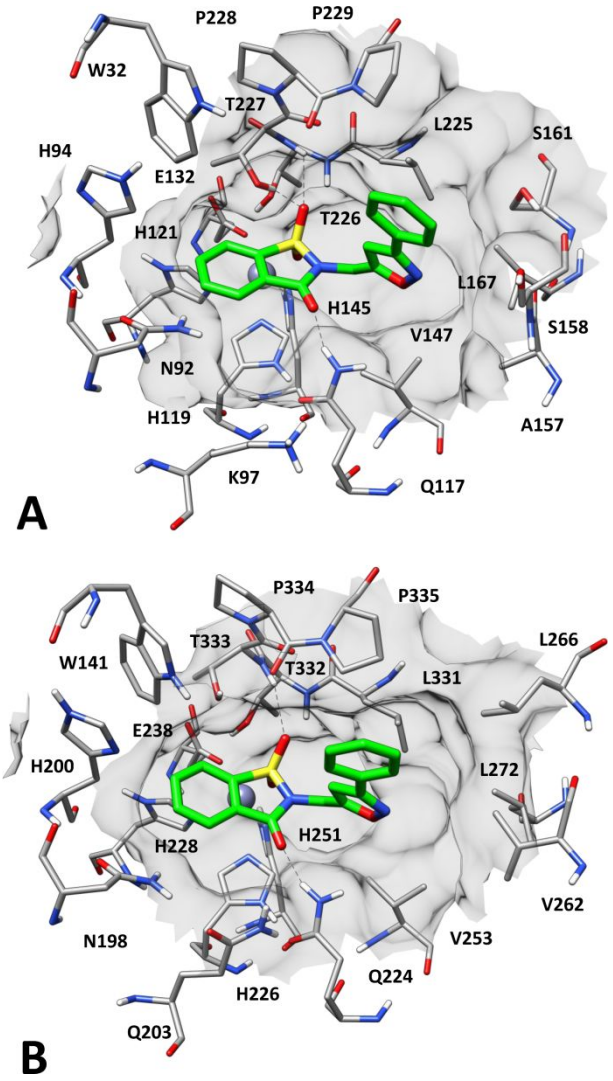

Figure 8. Minimized average structures of compound **8b** (green) in complex with (A) hCA XII (PBD code: 1JD0) and (B) hCA IX (PBD code: 3IAI). The protein surface surrounding the ligand is shown in grey.

In order to get insightful information on the selectivity profile of this series of ligands, the same docking protocol applied on hCA XII and hCA IX was also used to evaluate the potential binding mode of compound **8b** into hCA II and hCA I. The docking results suggested that the binding disposition described for the ligand into hCA XII and hCA IX could not be assumed into the other two CA isoforms, due to the steric hindrance of non-conserved residues. Precisely, the presence of F130 on the hydrophobic side of hCA II binding pocket, with its benzyl side chain oriented toward the centre of the catalytic site, would hamper the proper disposition of the ligand phenylisoxazole group, thus preventing the compound to assume the binding mode predicted into the tumour-related hCA isoforms (Figure S1). Differently, the presence of few non-conserved residues within the catalytic site of hCA I would totally occlude the small pocket where the phenyl ring of the ligand saccharin scaffold should be placed according to the binding mode predicted into hCA XII and hCA IX. In particular, the side chain of H201 of hCA I, that replaces the threonine residues T227 and T333 of hCA XII and hCA IX, respectively, is directed inside the pocket, thus preventing the binding of the ligand (Figure S2). These results and considerations could provide a possible explanation for rationalizing the selectivity profile of compound **8b** and the related series of compounds. Finally, the binding dispositions into hCA XII and hCA IX of the two enantiomers **(*R*)-8a** and **(*S*)-8a**, obtained by replacing the isoxazole ring of **8b** with an isoxazoline linker, were evaluated using the same computational protocol comprising docking and MD studies. The results obtained were consistent with the biological activities determines for the two compounds, since they showed a very similar binding mode into both hCA XII and hCA IX, which was also comparable to that predicted for their analogue **8b** into the two enzyme isoforms. As shown in Figure S3, the two **8a** enantiomers coordinate the zinc ion with their sulfonamide moiety and place the phenyl ring of the saccharin scaffold into the lipophilic pocket formed by W32, N92, H94, H119 and H121 in hCA XII and W141, N198, H200, Q203, H226 and H228 in hCA IX. The phenylisoxazoline group of both ligands is oriented toward the hydrophobic wall of the two enzymes and the same pattern of H-bond interactions predicted for **8b** can be observed, namely, a couple of H-bonds with the hydroxyl

group and the backbone nitrogen of T227/T333 (of hCA XII/IX) and a third H-bond with the side chain of Q117/Q224 (of hCA XII/IX). At present, we could not identify a satisfying rationale for explaining the reduced selectivity for hCA XII and hCA IX of compound **(*S*)-9a**, nor its increased activity against the two CA isoforms with respect to either its enantiomer **(*R*)-9a** or its close analogues **9b**, **8b** and **(*R/S*)-8a**. Further in-depth computational analyses will be carried out in order to investigate and rationalize this experimental evidence.

Biological evaluation on normal cells

According to the hCA inhibitory data reported in Table 1 and keeping in mind the possibility for nitro-containing molecules to be considered as "red flags" in Medicinal Chemistry, two compounds, **2b** and **7b**, were selected among the most potent as nanomolar hCA IX and XII inhibitors. More in detail, compounds **2b** and **7b** are characterized by a structurally similar skeleton (saccharin-isoxazoles), whereas they only differ for the presence of an electron-withdrawing moiety (NO_2 in **2b**) or an electron-donating group (OCH_3 in **7b**) at the *para* position of the aryl ring. They were tested in *in vitro* models, represented by both normal and tumoral cells, in order to evaluate the antiproliferative and cytotoxic effect of the two above mentioned compounds.

Firstly, compounds **2b** and **7b** were screened and tested on normal human cells represented by gingival fibroblasts (HGFs). Doses ranging from to 0.05 to 200 μM were selected administrating compounds **2b** and **7b** up to 72 h of culture. To evaluate the cytotoxicity, a Lactate Dehydrogenase (LDH) assay, which quantitatively measures LDH released upon cell lysis in the medium, was performed; 24, 48 and 72 h of culture were chosen as experimental times (Figure S24). Regarding compound **2b** (nitro-containing molecule), at all experimental times there are not statistically significant differences between the tested doses (Figure S24 A), conversely, when compound **7b** (methoxy-containing molecule) is administered, after 24 h of culture, a statistically significant reduction in LDH released % is recorded in HGFs treated with compound **7b** 200 μM and 100 μM with respect to control sample (DMSO) and to all other tested concentrations. After 48 and 72 h of

treatment with compound **7b** no significant differences are detected among the tested concentrations (Figure S24, B).

Secondly, after 24, 48 and 72 h of culture, a metabolic activity test (MTT assay), which is descriptive of cell viability rate, was performed on HGFs treated with compounds **2b** and **7b**. Again for compound **2b** no significant differences among the tested concentrations are recorded at all experimental times (Figure S25, A). Conversely, when HGFs are treated with compound **7b** a statistically significant decrease in viable cells % could be clearly evidenced after 24 and 48 h with 200, 100 and 50 μM doses with respect to cells treated with 5, 0.5, 0.05 μM and DMSO. After 72 h of culture, a decrease of viable cells % is detected only for cells treated with 200 and 100 μM compared to HGFs treated with 5, 0.5, 0.05 μM and to DMSO sample (Figure S25, B).

Taken together, these results clearly evidence that, in terms of both cytotoxicity and cell viability, the nitro-containing compound **2b** does not affect the pivotal biological processes occurring within the cells; in fact, even when administered at very high concentrations, the proliferation rate and the cytotoxic effect are comparable with control samples, thus indicating a good tolerability of molecule **2b** in normal cells. Concerning compound **7b**, it can be argued that an appreciable tolerability is recorded for doses lower than 50 μM, however, even when compound **7b** is administered at very high doses (100 and 200 μM), the cell viability never goes below 50% thus underlining a high safety profile despite the substitution pattern.

Biological evaluation on breast adenocarcinoma cells (MCF7)

Compounds **2b** and **7b** were then tested in a tumoral biological *in vitro* model represented by MCF7 breast adenocarcinoma cells. It is commonly recognized that breast cancer is as a chemoresistant tumor[25] and this often represents the main reason for inadequate therapeutic strategies. Considering that doxorubicin is a first-line drug for breast cancer therapy, we aimed at evaluating the co-treatment of compounds **2b** and **7b** with doxorubicin on MCF7 cells for 72 h. hCA IX and XII inhibitors were shown to counteract the overexpression of these cancer-related CA isozymes involved in tumor progression, metastasis development and angiogenesis in cancer cells adapted to

a hypoxic environment. For this reason, before administering compounds **2b** and **7b** in combination with doxorubicin, a pretreatment with $CoCl_2$ was carried out to induce hypoxia for 48 h. This approach is based on the well-established chemical induction of HIF-1α exerted by cobalt(II) chloride hexahydrate in order to overexpress CA IX and XII isozymes in MCF7 cells.

A dose–response evaluation, obtained by a MTT test and using doxorubicin doses ranging from 0.05 to 200 μM, was firstly performed aiming to select a subtoxic dose to be applied in combination with molecules **2b** and **7b** (Figure 9A). Given that our results show that, after 72 h of treatment, doxorubicin IC_{50} can be included between 50 and 5 μM, we chose 2.5 μM as a suitable subtoxic dose to be combined with **2b** and **7b** concentrations ranging from 0.05 to 200 μM.

MTT test, performed on MCF7 treated with compound **2b** + doxorubicin 2.5 μM for 72 h, discloses no statistically significant differences among the tested concentrations (Figure 9B). Whereas when MCF7 are treated with compound **7B** in combination with doxorubicin 2.5 μM for 72 h, a statistically significant reduction of viable cell percentage is recorded in 200 μM sample respect to all other experimental conditions. A similar trend is detectable for cells treated with 100 μM concentration with respect to 5, 0.5, 0.05 μM and control ($CoCl_2$ + DMSO) samples (Figure 9C). These data let us to hypothesize that probably MCF7 cells are chemoresistant to treatment performed with compound **2b**, even when combined with subtoxic doses of doxorubicin while the combination at high doses of compound **7b** with doxorubicin 2.5 μM could represent a chemosensitizer strategy to treat breast adenocarcinoma cells. To elucidate this hypothesis a morphological analysis, by means of phase contrast light microscope, was also carried out. The obtained results, shown in Figure 10, are quite surprising as taken pictures clearly show that MCF7 cells treated with compound **2b**, at both 100 and 200 μM, are round shaped, close to detachment, similarly to cells treated with compound **7b**. This could be explained admitting that MCF7 cells treated with compound **2b**, after 72 h, are still viable, as recognized by the viability assay (Figure 9), but they seem to be early affected by the compound. This led us to assume that compound **2b**, to affect the viability of tumoral cells, probably needs a longer treatment respect to compound **7b**.

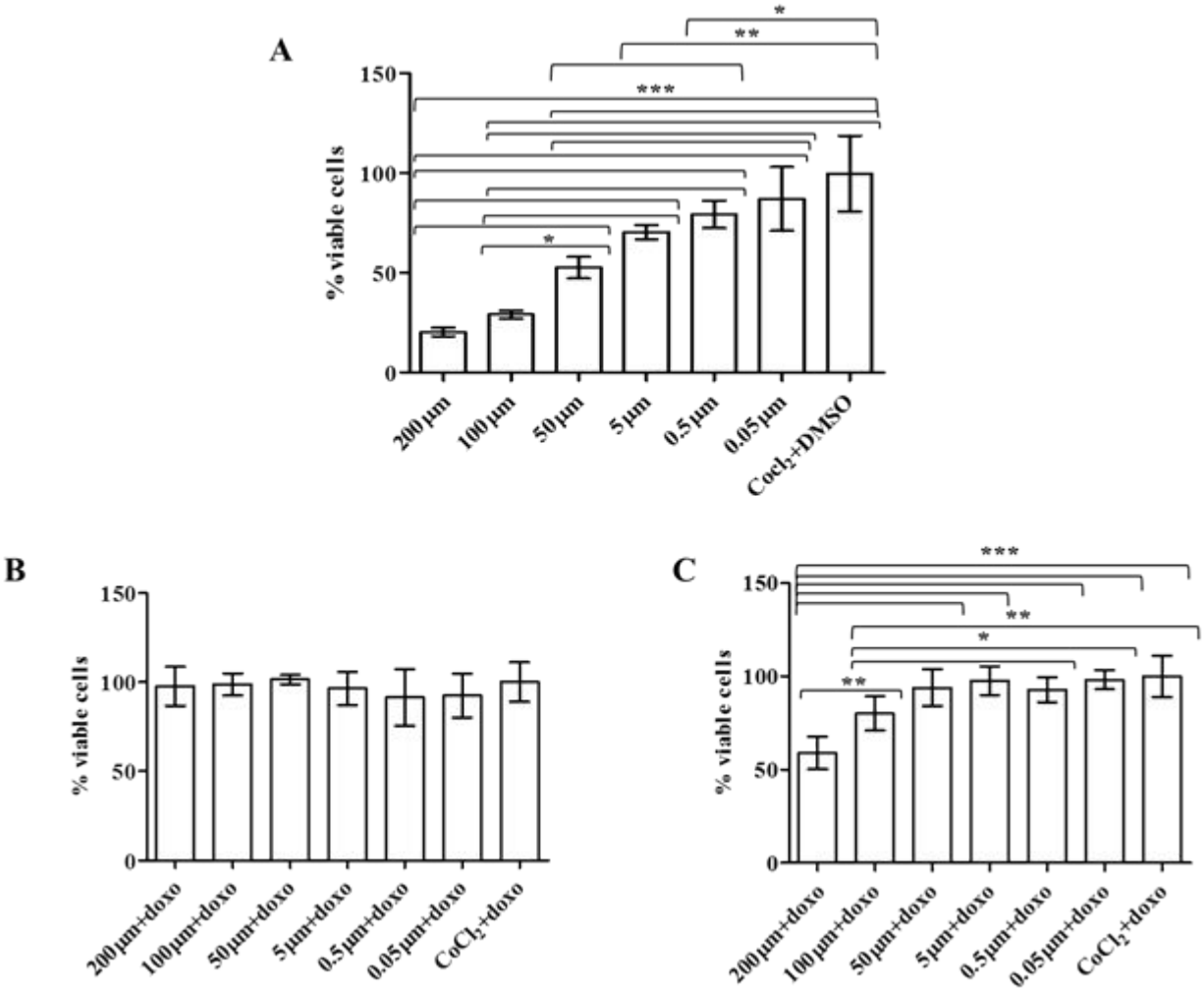

Figure 9. MTT cell viability assay on MCF7 cell line. **A** Histogram represents the viability dose-response of MCF7 cells exposed to different concentrations of doxorubicin (from 0.05 to 200 µM) for 72 h. **B** and **C** Histograms represent the viability dose-response of MCF7 cells exposed to different concentrations of compounds **2b** and **7b** (from 0.05 to 200 µM), respectively, in combination with doxorubicin 2.5 µM (subtoxic dose) for 72 h. Proliferation was assessed using MTT assay and normalized to control cells treated with DMSO (0.2% as final concentration) + $CoCl_2$ + doxorubicin 2.5 µM. The most representative of three separate experiments is shown. Data are presented as the mean ± standard deviation.

* $p<0.005$; ** $p<0.0005$; *** $p<0.0002$.

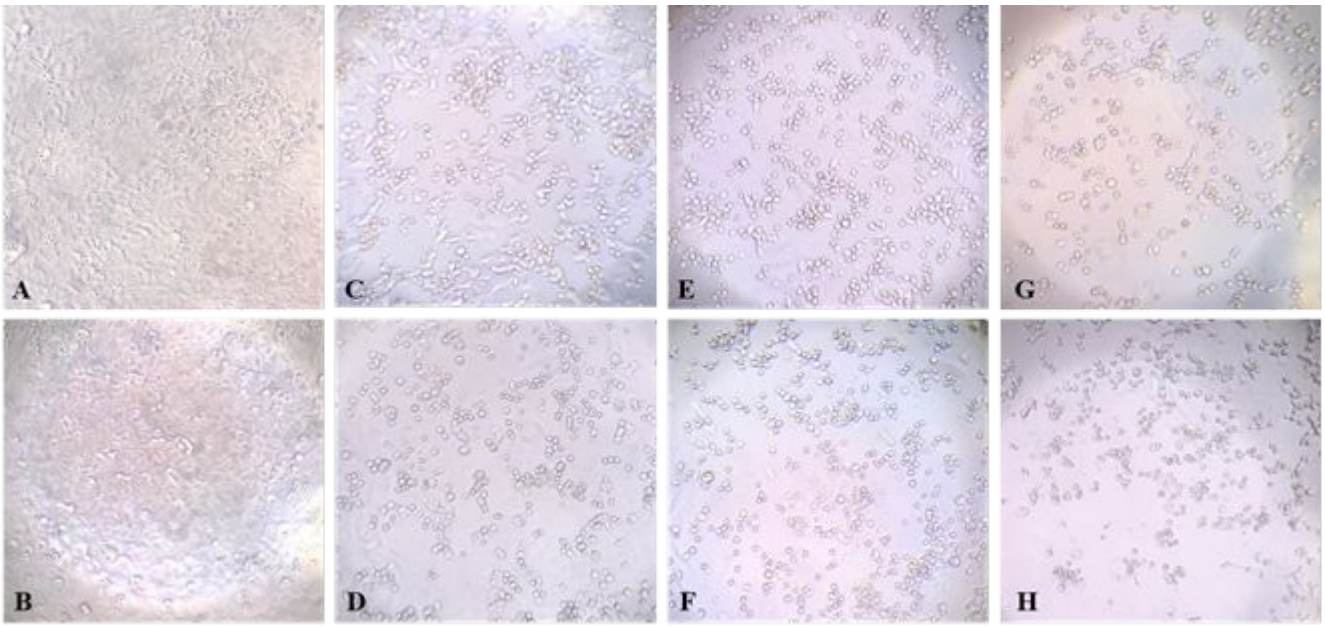

Figure 10. Phase contrast microscopy images of MCF7 cells treated with doxorubicin, compounds **2b** and **7b** for 72 h. **A**: DMSO, **B**: DMSO + $CoCl_2$, **C**: Doxorubicin 2.5 μM, **D**: Doxorubicin 5 μM; **E**: **2b** 100 μM + doxorubicin 2.5 μM, **F**: **2b** 200 μM + doxorubicin 2.5 μM, **G**: **7b** 100 μM + doxorubicin 2.5 μM, **H**: **7b** 200 μM + doxorubicin 2.5 μM. Adherent and viable cells are detectable in samples **A** and **B**, whereas a high number of detached and floating cells is appreciable in all other experimental points, particularly in samples **G** and **H**. Magnification ×20.

Considering that doxorubicin is very efficient *in vitro*, when given as monotherapy, but can be cardiotoxic *in vivo* at therapeutic levels, our results confirmed the putative role of hCA IX and XII inhibitors as chemosensitizers or coadjuvants to reduce antitumoral drug concentration and thus limiting the possibility to develop harmful side effects. In addition, there is a strong need to develop combined therapies to define synergistic or additive actions improving the therapeutic index of the therapy or decrease adaptive resistance.

Conclusions

In this paper we report on the development of two series of potent and selective hCAs inhibitors based on the well-established saccharin scaffold. On the basis of the previously reported "tail approach", we explored the introduction of isoxazole and isoxazoline linkers for the decoration of saccharin cyclic sulfonamide. In fact, *in silico* studies suggested that a phenyl-isoxazole moiety could be important for the establishment of pivotal interactions with the lipophilic side of the catalytic site, while the sulfonamide fragment was predicted to be responsible of both zinc coordination and H-bonds formation with key anchoring residues. *In vitro* results evidenced that compounds belonging to both series were characterised by strong affinity for hCA IX and XII and marked selectivity over hCA I and II. Moreover, two of the newly synthesised compounds were submitted to HPLC enantioseparation to assess the enzyme ability to discriminate between the two enantiomers.

It is also worth noting that two of the most potent nanomolar hCA IX and XII inhibitors did not displayed any cytotoxic effect up to 200 μM on primary human fibroblasts despite the substitution pattern (nitro or methoxy moiety), whereas compound **7b** was shown to act as chemosensitizer and coadjuvant in combination with subtoxic doses of doxorubicin on MCF7 breast cancer cell line. Overall, these *in vitro* activity data are encouraging for further future development of this scaffold.

Experimental protocols

Chemistry

Unless otherwise indicated, all reactions were carried out under a positive pressure of nitrogen (balloon pressure) in washed and oven-dried glassware. Solvents were used as supplied without further purification. Where mixtures of solvents are specified, the stated ratios are volume:volume. Reagents for the chemical and biological experiments were used directly as supplied by Sigma-Aldrich® Italy, unless otherwise stated. All melting points were measured on a Stuart® melting point apparatus SMP1, and are uncorrected. Temperatures are reported in °C. ^{1}H and ^{13}C NMR spectra were recorded at 400 and 101 MHz, respectively, on a Bruker spectrometer using $CDCl_3$, DMSO-d_6, CD_3OD and CD_3CN, as the solvents at room temperature. The samples were analysed with a final concentration of ~30 mg/mL. Chemical shifts are expressed as δ units (parts per millions) relative to the solvent signal. ^{1}H spectra are described as follows: δ_H (spectrometer frequency, solvent): chemical shift/ppm (multiplicity, J-coupling constant(s), number of protons, assignment). ^{13}C spectra are described as follows: δ_C (spectrometer frequency, solvent): chemical shift/ppm (assignment). Multiplets are abbreviated as follows: br – broad; s – singlet; d – doublet; t – triplet; q – quartet; m – multiplet. Coupling constants J are valued in Hertz (Hz). Infra-red spectra were recorded on a Bruker Tensor 27 FTIR spectrometer equipped with an attenuated total reflectance attachment with internal calibration. Absorption maxima (ν_{max}) are reported in wavenumbers (cm^{-1}). Column chromatography was carried out using Sigma-Aldrich® silica gel (high purity grade, pore size 60 Å, 230-400 mesh particle size). All the purifications and reactions were carried out by TLC performed on 0.2 mm thick silica gel-aluminium backed plates (60 F254, Merck). Visualization was performed under ultra-violet irradiation (254 and 365 nm). Where given, systematic compound names are those generated by ChemBioDraw Ultra 12.0 following IUPAC conventions.

The purity of all final compounds was >95% as determined by HPLC analyses performed using the Shimadzu *Prominence-i* LC-2030C 3D system, that integrates autosampler, binary pump, column oven and a photodiode array detector (PDA). The separation was performed using the column Kinetex Evo C18, 5 µm, 100 Å (Phenomenex, Bologna, Italy) at a constant flow of 1.25 mL min^{-1},

employing a binary mobile phase elution gradient. The two eluents used were water (solvent A) and acetonitrile (solvent B) mixed in different elution gradients for isoxazole and isoxazoline derivatives. For the compounds endowed with an isoxazole moiety the initial eluent composition was 50% of solvent B. This concentration has been kept constant for 3 min, then raised up to 90% in 7 min and maintained at this value for 1 min. At the end of this time the concentration returned at the initial value for the column reconditioning (4 min), to a total run time of 15 min (chromatograms are reported as Supporting Information).

For the derivatives bearing the isoxazole moiety the chromatographic run started with 30% of solvent B, that also in this case was kept constant for 3 min. The concentration was then raised up to 90% in 7 min, and maintained at this value for 1 min. After this time the concentration returned at the initial value for the column reconditioning (4 min), to a total run time of 15 min. With the exception of compound **2a** which exhibited scarce solubility, all the analyte solutions were prepared in acetonitrile at the concentration of about 1 mg mL^{-1}, and 2 μL were directly injected for the HPLC analysis. All compounds reported were ≥ 95% HPLC pure. The solvents used in the HPLC analysis were acetonitrile, purchased from Carlo Erba Reagents and mQ water 18 MΩ cm, obtained from Millipore's Direct-Q3 system.

*Synthesis and characterization data for saccharin derivatives **S1-S2***

*2-Allylbenzo[d]isothiazol-3(2H)-one 1,1-dioxide (**S1**) and 2-(prop-2-yn-1-yl)-1,2-benzothiazol-3(2H)-one 1,1-dioxide **S2***. See reference [17] for synthesis procedure and characterization data.

*Synthesis and characterization data for oximes **O1-O9***

*3-Nitrobenzaldehyde oxime **O1***. In an oven-dried flask, hydroxylamine hydrochloride (1.0 g, 0.014 mol) and triethylamine (3.0 mL, 0.021 mol) were dissolved in 10 mL of anhydrous methanol and stirred for 5 min at room temperature. 3-Nitrobenzaldehyde (1.45 g, 0.0096 mol) was added and the reaction mixture stirred at 80 °C until complete consumption of the starting material. The reaction was cooled down to room temperature and the solvent removed *in vacuo*. 20 mL of ice-cold water were added to the residue and the resulting suspension was kept at 0-4 °C overnight in order to

obtain oxime precipitate, which was filtered and washed with a mixture of petroleum ether/diethyl ether, obtaining the title compound as a light yellow solid (1.35 g, 85% yield). See reference [26] for characterization data.

4-Nitrobenzaldehyde oxime ***O2***. See reference [17] for synthesis procedure and characterization data.

Pyridine-2-aldoxime ***O3***. In an oven-dried flask, hydroxylamine hydrochloride (1.0 g, 0.014 mol) and triethylamine (3.0 mL, 0.021 mol) were dissolved in 10 mL of anhydrous methanol and stirred for 5 min at room temperature. Pyridine-2-carboxaldehyde (0.92 mL, 0.0096 mol) was added and the reaction mixture stirred at 80 °C until complete consumption of the starting material. The reaction was cooled down to room temperature and the solvent removed *in vacuo*. 20 mL of ice-cold water were added to the residue and the resulting suspension was kept at 0-4 °C overnight in order to obtain oxime precipitate, which was filtered and washed with a mixture of petroleum ether/diethyl ether, obtaining the title compound as a white solid (0.82 g, 70% yield). See reference [27] for characterization data.

Pyridine-3-aldoxime ***O4***. In an oven-dried, flask hydroxylamine hydrochloride (1.0 g, 0.014 mol) and triethylamine (3.0 mL, 0.021 mol) were dissolved in 10 mL of anhydrous methanol and stirred for 5 min at room temperature. Pyridine-3-carboxaldehyde (0.90 mL, 0.0096 mol) was added and the reaction mixture stirred at 80 °C until complete consumption of the starting material. The reaction was cooled down to room temperature and the solvent removed *in vacuo*. 20 mL of ice-cold water were added to the residue and the resulting suspension was kept at 0-4 °C overnight in order to obtain oxime precipitate, which was filtered and washed with a mixture of petroleum ether/diethyl ether, obtaining the title compound as a white solid (1.07 g, 92% yield). See reference [28] for characterization data.

2-Methoxybenzaldehyde oxime ***O5***. In an oven-dried, flask hydroxylamine hydrochloride (1.0 g, 0.014 mol) and triethylamine (3.0 mL, 0.021 mol) were dissolved in 10 mL of anhydrous methanol and stirred for 5 min at room temperature. 2-Methoxybenzaldehyde (1.30 g, 0.0096 mol) was added

and the reaction mixture stirred at 80 °C until complete consumption of the starting material. The reaction was cooled down to room temperature and the solvent removed *in vacuo*. 20 mL of ice-cold water were added to the residue and the resulting suspension was kept at 0-4 °C overnight in order to obtain oxime precipitate, which was filtered and washed with a mixture of petroleum ether/diethyl ether, obtaining the title compound as a light yellow solid (1.29 g, 89% yield). See reference [26] for characterization data.

3-Methoxybenzaldehyde oxime ***O6***. In an oven-dried, flask hydroxylamine hydrochloride (1.0 g, 0.014 mol) and triethylamine (3.0 mL, 0.021 mol) were dissolved in 10 mL of anhydrous methanol and stirred for 5 min at room temperature. 3-Methoxybenzaldehyde (1.30 g, 0.0096 mol) was added and the reaction mixture stirred at 80 °C until complete consumption of the starting material. The reaction was cooled down to room temperature and the solvent removed *in vacuo*. 20 mL of ice-cold water were added to the residue and the resulting suspension was extracted with ethyl acetate (3 x 20 mL). The organics were reunited, dried over sodium sulphate and evaporated *in vacuo* to give the title compound as thick oil (1.27 g, 88% yield). See reference [26] for characterization data.

4-Methoxybenzaldehyde oxime **O7**. In an oven-dried flask, hydroxylamine hydrochloride (1.0 g, 0.014 mol) and triethylamine (3.0 mL, 0.021 mol) were dissolved in 10 mL of anhydrous methanol and stirred for 5 min at room temperature. 4-Methoxybenzaldehyde (1.30 g, 0.0096 mol) was added and the reaction mixture stirred at 80 °C until complete consumption of the starting material. The reaction was cooled down to room temperature and the solvent removed *in vacuo*. 20 mL of ice-cold water were added to the residue and the resulting suspension was kept at 0-4 °C overnight in order to obtain oxime precipitate, which was filtered and washed with a mixture of petroleum ether/diethyl ether, obtaining the title compound as a white solid (1.29 g, 89% yield). See reference [26] for characterization data.

Benzaldehyde oxime ***O8***. In an oven-dried flask, hydroxylamine hydrochloride (1.0 g, 0.014 mol) and triethylamine (3.0 mL, 0.021 mol) were dissolved in 10 mL of anhydrous methanol and stirred for 5 min at room temperature. Benzaldehyde (0.97 mL, 0.0096 mol) was added and the reaction

mixture stirred at 80 °C until complete consumption of the starting materials. The reaction was cooled down to room temperature and the solvent removed *in vacuo*. 20 mL of ice-cold water were added to the residue and the resulting suspension was extracted with ethyl acetate (3 x 20 mL). The organics were reunited, dried over sodium sulphate and evaporated *in vacuo* to give the title compound as colourless oil (0.87 g, 75% yield). See reference [26] for characterization data.

Thiophene-2-carbaldehyde oxime ***O9***. In an oven-dried flask, hydroxylamine hydrochloride (1.0 g, 0.014 mol) and triethylamine (3.0 mL, 0.021 mol) were dissolved in 10 mL of anhydrous methanol and stirred for 5 min at room temperature. Thiophene-2-carbaldehyde (1.07 g, 0.0096 mol) was added and the reaction mixture stirred at 80 °C until complete consumption of the starting materials. The reaction was cooled down to room temperature and the solvent removed *in vacuo*. 20 mL of ice-cold water were added to the residue and the resulting suspension was kept at 0-4 °C overnight in order to obtain oxime precipitate, which was filtered and washed with a mixture of petroleum ether/diethyl ether, obtaining the title compound as a light brown solid (0.77 g, 63% yield). See reference [27] for characterization data.

Synthesis and characterization data for chloro oximes ***C1-C9***

N-hydroxy-3-nitrobenzimidoyl chloride ***C1***. In an oven-dried flask, *m*-nitrobenzaldoxime **O1** (1 g, 0.006 mol) was dissolved in 10 mL of anhydrous DMF. *N*-chlorosuccinimide (0.16 g, 0.0012 mol) was added and the reaction stirred for 10 min at room temperature. The solution was purged with 20 mL of $HCl_{(g)}$, stirred for 10 additional min and then heated up to 50 °C. *N*-chlorosuccinimide was added portionwise (0.16 g or 0.0012 mol at the time, up to 1.20 g or 0.009 mol) over half an hour. The progression of the reaction was monitored using iodine starch paper. When the iodine starch paper was not turning brown anymore, the reaction was quenched with 4 volumes of ice-cold water. The aqueous phase was extracted with diethyl ether (3 x 20 mL), the organics reunited were dried over sodium sulphate and evaporated *in vacuo* to give the title compound as a yellow-orange solid (0.83 g, 69% yield). See reference [29] for characterization data.

N-hydroxy-4-nitrobenzimidoyl chloride ***C2***. See reference [17] for the synthesis procedure and characterization data.

N-hydroxy-pyridine-2-carbimidoyl chloride ***C3***. In an oven-dried flask, pyridine-2-aldoxime **O3** (1 g, 0.008 mol) was treated as compound **O1** to give the title compound as a light brown solid (0.97 g, 76% yield). See reference [30] for the synthesis and characterization data.

N-hydroxy-pyridine-3-carbimidoyl chloride ***C4***. In an oven-dried flask, pyridine-3-aldoxime **O4** (1 g, 0.008 mol) was treated as compound **O1** to give the title compound as brown solid (1.10 g, 88% yield). See reference [29] for the synthesis and characterization data.

N-hydroxy-2-methoxybenzimidoyl chloride ***C5***. In an oven-dried flask, 2-methoxybenzaldehyde oxime **O5** (1 g, 0.007 mol) was treated as compound **O1** to give the title compound as a white solid (0.99 g, 81% yield). See reference [31] for the characterization data.

N-hydroxy-3-methoxybenzimidoyl chloride ***C6***. In an oven-dried, flask 3-methoxybenzaldehyde oxime **O6** (1 g, 0.007 mol) was treated as compound **O1** to give the title compound as a yellow oil (0.99 g, 81% yield); ^{1}H-NMR (400 MHz, $CDCl_3$): δ 3.81 (s, 3H, OCH_3), 6.93-6.98 (m, 1H, Ar), 7.25-7.30 (m, 2H, Ar), 7.38-7.44 (m, 1H, Ar), 10.84 (br, 1H, OH, D_2O exch.).

N-hydroxy-4-methoxybenzimidoyl chloride ***C7***. In an oven-dried, flask 4-methoxybenzaldehyde oxime **O7** (1 g, 0.007 mol) was treated as compound **O1** to give the title compound as a yellow solid (0.71 g, 58% yield). See reference [32] for the characterization data.

N-hydroxybenzimidoyl chloride ***C8***. In an oven-dried flask, benzaldoxime **O8** (1 g, 0.008 mol) was treated as compound **O1** to give the title compound as a yellow oil (0.83, 65% yield). See reference [28] for the characterization data.

N-hydroxythiophene-2-carbimidoyl chloride ***C9***. In an oven-dried, flask thiophene-2-carbaldehyde oxime **O9** (1 g, 0.008 mol) was treated as compound **O1** to give the title compound as a green solid (0.80 g, 64% yield). See reference [31] for the characterization data.

Synthesis and characterization data for saccharin/isoxazoline derivatives ***1a-9a***

2-((3-(3-Nitrophenyl)-4,5-dihydroisoxazol-5-yl)methyl)benzo[d]isothiazol-3(2H)-one 1,1-dioxide ***1a***. 2-Allylbenzo[*d*]isothiazol-3(*2H*)-one 1,1-dioxide **S1** (1 g, 0.0044 mol) and *N*-hydroxy-3-nitrobenzimidoyl chloride **C1** (1.10 g, 0.0055 mol) were dissolved in 50 mL of anhydrous ethyl acetate. Triethylamine (0.76 mL, 0.0055 mol) in ethyl acetate was added dropwise over 30 min. A white suspension was formed and stirred overnight at room temperature. The reaction was quenched with 40 mL of water and the resulting suspension was extracted with dichloromethane (3 x 20 mL). The organics reunited were dried over sodium sulphate and evaporated *in vacuo* to give the title compound as a light yellow solid (1.34 g, 77% yield); mp 175–177 °C; IR ν_{max} 3088 (ν C_{sp2}-H), 1744 (ν C=O), 1593 (ν C=N), 1525 (ν_{as} NO_2), 1343 (ν_s NO_2), 1323 (ν_{as} S=O), 1302 (ν NO_2), 1263 (ν C-N), 1177 (ν_s S=O), 719 (δ C_{sp2}-H), 674 (δ C_{sp2}-H) cm^{-1}. ^{1}H-NMR (400 MHz, DMSO-d_6): δ 3.44 (dd, ^2J = 17.2 Hz, ^3J = 6.6 Hz, 1H C(4)H_2-isoxazoline), 3.68 (dd, ^2J = 17.0 Hz, ^3J = 11.0 Hz, 1H, C(4)H_2-isoxazoline), 3.90 (dd, ^2J = 15.2 Hz, ^3J = 4.4 Hz, 1H, CH_2), 4.03 (dd, ^2J = 15.2 Hz, ^3J = 7.2 Hz, 1H, CH_2), 5.14-5.21 (m, 1H, C(5)H-isoxazoline), 7.73-7.77 (m, 1H, Ar), 7.98-8.13 (m, 4H, Ar), 8.29-8.33 (m, 2H, Ar), 8.37 (s, 1H, Ar). ^{13}C-NMR (101 MHz, $CDCl_3$): δ 38.3 (C(4)H_2-isoxazoline), 41.5 (CH_2), 78.3 (C(5)H-isoxazoline), 121.2 (Ar), 121.7 (Ar), 124.8 (Ar), 125.5 (Ar), 126.9 (Ar), 129.9 (Ar), 130.9 (Ar), 132.4 (Ar), 134.6 (Ar), 135.2 (Ar), 137.5 (Ar), 148.5 (Ar), 154.9 (C=N, isoxazoline), 159.4 (C=O).

2-((3-(4-Nitrophenyl)-4,5-dihydroisoxazol-5-yl)methyl)benzo[d]isothiazol-3(2H)-one 1,1-dioxide ***2a***. 2-Allylbenzo[*d*]isothiazol-3(*2H*)-one 1,1-dioxide **S1** (1 g, 0.0044 mol) and *N*-hydroxy-4-nitrobenzimidoyl chloride **C2** (1.10 g, 0.0055 mol) were dissolved in 50 mL of anhydrous ethyl acetate. Triethylamine (0.76 mL, 0.0055 mol) in ethyl acetate was added dropwise over 30 min. A white suspension was formed and stirred overnight at room temperature. The reaction was quenched with 40 mL of water and the resulting suspension was filtered to give title compound as a light yellow solid (1.11 g, 64% yield); mp 210-213 °C; IR ν_{max} 3076 (ν C_{sp2}-H), 1735 (ν C=O), 1580 (ν C=N), 1509 (ν_{as} N-O), 1326 (ν_{as} S=O), 1308 (ν_s N-O), 1247 (ν C-N), 1181 (ν_s S=O), 849 (δ C_{sp2}-H), 749 (δ C_{sp2}-H) cm^{-1}. ^{1}H-NMR (400 MHz, DMSO-d_6): δ 3.41 (dd, ^2J = 16.2 Hz, ^3J = 7.2 Hz, 1H

C(4)H_2-isoxazoline), 3.66 (dd, ^2J =17.6 Hz, ^3J = 10.8 Hz, 1H, C(4)H_2-isoxazoline), 3.91 (dd, ^2J = 15.4 Hz, ^3J = 4.6 Hz, 1H, CH_2), 4.04 (dd, ^2J = 15.2 Hz, ^3J = 7.2 Hz, 1H, CH_2), 5.17-5.19 (m, 1H, C(5)H-isoxazoline), 7.90 (d, J = 8.4 Hz, 2H, Ar), 8.00-8.12 (m, 3H, Ar), 8.27-8.32 (m, 3H, Ar). ^{13}C-NMR (101 MHz, DMSO-d_6): δ 38.0 (C(4)H_2, isoxazoline), 42.1 (CH_2), 79.0 (C(5)H-isoxazoline), 122.1 (Ar), 124.5 (2 x Ar), 125.7 (Ar), 126.6 (Ar), 128.3 (2 x Ar), 135.7 (Ar), 135.8 (Ar), 136.4 (Ar), 137.2 (Ar), 148.5 (Ar), 156.4 (C=N, isoxazoline), 159.4 (C=O).

2-((3-(Pyridin-2-yl)-4,5-dihydroisoxazol-5-yl)methyl)benzo[d]isothiazol-3(2H)-one 1,1-dioxide ***3a***. 2-Allylbenzo[*d*]isothiazol-3(*2H*)-one 1,1-dioxide **S1** (1 g, 0.0044 mol) and *N*-hydroxy-pyridine-2-carbimidoyl chloride **C3** (0.86 g, 0.0055 mol) were dissolved in 50 mL of anhydrous ethyl acetate. Triethylamine (0.76 mL, 0.0055 mol) in ethyl acetate was added dropwise over 30 min. A white suspension was formed and stirred overnight at room temperature. The reaction was quenched with 40 mL of water and the resulting suspension was extracted with dichloromethane (3 x 20 mL). The organics reunited were dried over sodium sulphate and evaporated *in vacuo* to give the title compound as a light orange solid (1.49 g, 97% yield); mp 133-135 °C; IR ν_{max} 2928 (ν C_{sp2}-H), 1739 (ν C=O), 1578 (ν C=N), 1320 (ν_{as} S=O), 1300 (ν N-O), 1288 (ν C-N), 1173 (ν_s S=O), 778 (δ C_{sp2}-H), 745 (δ C_{sp2}-H) cm^{-1}. ^{1}H-NMR (400 MHz, DMSO-d_6): δ 3.39-3.45 (m, 1H C(4)H_2-isoxazoline), 3.59-3.66 (m, 1H, C(4)H_2-isoxazoline), 3.89-3.94 (m, 1H, CH_2), 3.99-4.04 (m, 1H, CH_2), 5.11-5.12 (m, 1H, C(5)H-isoxazoline), 7.42-7.45 (m, 1H, pyr), 7.84-7.92 (m, 1H Ar + 1H pyr), 7.97-8.11 (m, 2H Ar + 1H pyr), 8.30-8.32 (m, 1H, Ar), 8.61 (s, 1H, pyr). ^{13}C-NMR (101 MHz, DMSO-d_6): δ 38.4 (C(4)H_2-isoxazoline), 42.2 (CH_2), 78.5 (C(5)H-isoxazoline), 121.8 (pyr), 122.1 (Ar), 125.2 (pyr), 125.7 (Ar), 126.6 (pyr), 135.8 (Ar), 136.4 (Ar), 137.1 (Ar), 137.4 (pyr), 148.9 (Ar), 149.9 (pyr), 158.9 (C=N, isoxazoline), 159.4 (C=O).

2-((3-(Pyridin-3-yl)-4,5-dihydroisoxazol-5-yl)methyl)benzo[d]isothiazol-3(2H)-one 1,1-dioxide ***4a***. 2-Allylbenzo[*d*]isothiazol-3(*2H*)-one 1,1-dioxide **S1** (1 g, 0.0044 mol) and *N*-hydroxy-pyridine-3-carbimidoyl chloride **C4** (0.86 g, 0.0055 mol) were dissolved in 50 mL of anhydrous ethyl acetate. Triethylamine (0.76 mL, 0.0055 mol) in ethyl acetate was added dropwise over 30 min. A white

suspension was formed and stirred overnight at room temperature. The reaction was quenched with 40 mL of water and the resulting suspension was extracted with dichloromethane (3 x 20 mL). The organics reunited were dried over sodium sulphate and evaporated *in vacuo.* Purification by column chromatography on silica gel (ethyl acetate:*n*-hexane 1:1) gave the title compound as a light orange solid (0.96 g, 62% yield); mp 98-100 °C; IR ν_{max} 3041 (ν C_{sp2}-H), 1733 (ν C=O), 1596 (ν C=N), 1335 (ν_{as} S=O), 1301 (ν N-O), 1260 (ν C-N), 1180 (ν_s S=O), 748 (δ C_{sp2}-H), 673 (δ C_{sp2}-H) cm^{-1}. ^{1}H-NMR (400 MHz, $CDCl_3$): *δ* 3.31 (dd, ^2J = 17.0 Hz, ^3J = 6.6 Hz, 1H, C(4)H_2-isoxazoline), 3.45 (dd, ^2J =17.0 Hz, ^3J = 10.6 Hz, 1H, C(4)H_2-isoxazoline), 3.86 (dd, ^2J = 14.8 Hz, ^3J = 6.8 Hz, 1H, CH_2), 3.99 (dd, ^2J = 15.0 Hz, ^3J = 5.8 Hz, 1H, CH_2), 5.16-5.23 (m, 1H, C(5)H-isoxazoline), 7.24-7.27 (m, 1H, pyr), 7.76-7.88 (m, 2H Ar + 1 H pyr), 7.86-7.98 (m, 1H Ar + 1H pyr), 8.53-8.54 (m, 1H, Ar), 8.74-8.75 (m, 1H, pyr). ^{13}C-NMR (101 MHz, $CDCl_3$): *δ* 38.4 (C(4)H_2-isoxazoline), 41.6 (CH_2), 79.2 (C(5)H-isoxazoline), 121.1 (Ar), 123.6 (pyr), 125.3 (pyr), 125.4 (Ar), 126.8 (Ar), 133.9 (pyr), 134.6 (Ar), 135.2 (pyr), 137.3 (Ar), 147.8 (Ar), 151.1 (pyr), 154.3 (C=N, isoxazoline), 159.3 (C=O).

2-((3-(2-Methoxyphenyl)-4,5-dihydroisoxazol-5-yl)methyl)benzo[d]isothiazol-3(2H)-one 1,1-dioxide ***5a***. 2-Allylbenzo[*d*]isothiazol-3(*2H*)-one 1,1-dioxide **S1** (1 g, 0.0044 mol) and *N*-hydroxy-2-methoxybenzimidoyl chloride **C5** (1.02 g, 0.0055 mol) were dissolved in 50 mL of anhydrous ethyl acetate. Triethylamine (0.76 mL, 0.0055 mol) in ethyl acetate was added dropwise over 30 min. A white suspension was formed and stirred overnight at room temperature. The reaction was quenched with 40 mL of water and the resulting suspension was extracted with dichloromethane (3 x 20 mL). The organics reunited were dried over sodium sulphate and evaporated *in vacuo.* Purification by column chromatography on silica gel (ethyl acetate:*n*-hexane 1:1) gave the title compound as a white solid (1.10 g, 66% yield); mp 138-140 °C; IR ν_{max} 2940 (ν C_{sp2}-H), 1735 (ν C=O), 1333 (ν_{as} S=O), 1599 (ν C=N), 1302 (ν N-O), 1256 (ν C-N), 1174 (ν_s S=O), 770 (δ C_{sp2}-H), 753 (δ C_{sp2}-H) cm^{-1}. ^{1}H-NMR (400 MHz, $CDCl_3$): *δ* 3.51 (dd, ^2J = 17.8 Hz, ^3J = 6.2 Hz, 1H, C(4)H_2-isoxazoline), 3.60 (dd, ^2J =17.8 Hz, ^3J = 10.2 Hz, 1H, C(4)H_2-isoxazoline), 3.86-3.93 (m,

3H OCH_3 + 1H CH_2), 4.05 (dd, ^2J = 14.8 Hz, ^3J = 6.0 Hz, 1H, CH_2), 5.16-5.23 (m, 1H, C(5)H-isoxazoline), 6.93-7.00 (m, 2H, Ar), 7.37-7.41 (m, 1H, Ar), 7.73- 7.75 (m, 1H, Ar), 7.84-7.96 (m, 3H, Ar), 8.08 (d, ^3J = 7.6 Hz, 1H, Ar). ^{13}C-NMR (101 MHz, $CDCl_3$): δ 41.4 (C(4)H_2-isoxazoline), 41.9 (CH_2), 55.5 (OCH_3), 77.2 (C(5)H-isoxazoline), 111.4 (Ar), 118.3 (Ar), 120.8 (Ar), 121.1 (Ar), 125.4 (Ar), 127.1 (Ar), 129.6 (Ar), 131.5 (Ar), 134.5 (Ar), 135.1 (Ar), 137.5 (Ar), 156.1 (C=N, isoxazoline), 157.6 (Ar), 159.3 (C=O).

2-((3-(3-Methoxyphenyl)-4,5-dihydroisoxazol-5-yl)methyl)benzo[d]isothiazol-3(2H)-one 1,1-dioxide ***6a***. 2-Allylbenzo[*d*]isothiazol-3(*2H*)-one 1,1-dioxide **S1** (1 g, 0.0044 mol) and *N*-hydroxy-3-methoxybenzimidoyl chloride **C6** (1.02 g, 0.0055 mol) were dissolved in 50 mL of anhydrous ethyl acetate. Triethylamine (0.76 mL, 0.0055 mol) in ethyl acetate was added dropwise over 30 min. A white suspension was formed and stirred overnight at room temperature. The reaction was quenched with 40 mL of water and the resulting suspension was extracted with dichloromethane (3 x 20 mL). The organics reunited were dried over sodium sulphate and evaporated *in vacuo.* Purification by column chromatography on silica gel (ethyl acetate:petroleum ether 1:3) gave the title compound as a highly thick oil (1.36 g, 81% yield); IR ν_{max} 2938 (ν C_{sp2}-H), 1727 (ν C=O), 1595 (ν C=N), 1330 (ν_{as} S=O), 1301 (ν N-O), 1254 (ν C-N), 1183(ν_s S=O), 765 (δ C_{sp2}-H), 673 (δ C_{sp2}-H) cm^{-1}. ^{1}H-NMR (400 MHz, $CDCl_3$): δ 3.32-3.36 (m, 1H, C(4)H_2-isoxazoline), 3.43-3.50 (m, 1H, C(4)H_2-isoxazoline), 3.78-3.80 (m, 3H, OCH_3), 3.87-3.92 (m, 1H, CH_2), 4.02-4.06 (m, 1H, CH_2), 5.20 (br s, 1H, C(5)H-isoxazoline), 6.93-6.95 (m, 1H, Ar), 7.18-7.28 (m, 3H, Ar), 7.83-7.91 (m, 3H, Ar), 8.02-8.04 (m, 1H, Ar). ^{13}C-NMR (101 MHz, $CDCl_3$): δ 38.8 (C(4)H_2-isoxazoline), 41.8 (CH_2), 55.4 (OCH_3), 77.2 (C(5)H-isoxazoline), 111.5 (Ar), 116.6 (Ar), 119.5 (Ar), 121.1 (Ar), 125.4 (Ar), 126.9 (Ar), 129.8 (Ar), 130.3 (Ar), 134.6 (Ar), 135.2 (Ar), 137.4 (Ar), 156.5 (C=N, isoxazoline), 159.3 (Ar), 159.7 (C=O).

2-((3-(4-Methoxyphenyl)-4,5-dihydroisoxazol-5-yl)methyl)benzo[d]isothiazol-3(2H)-one 1,1-dioxide ***7a***. 2-Allylbenzo[*d*]isothiazol-3(*2H*)-one 1,1-dioxide **S1** (1 g, 0.0044 mol) and *N*-hydroxy-4-methoxybenzimidoyl chloride **C7** (1.02 g, 0.0055 mol) were dissolved in 50 mL of anhydrous

ethyl acetate. Triethylamine (0.76 mL, 0.0055 mol) in ethyl acetate was added dropwise over 30 min. A white suspension was formed and stirred overnight at room temperature. The reaction was quenched with 40 mL of water and the resulting suspension was filtered to give title compound as a white solid (1.20 g, 72% yield); mp 148-153 °C; IR ν_{max} 3069 (ν C_{sp2}-H), 1740 (ν C=O), 1607 (ν C=N), 1321 (ν_{as} S=O), 1301 (ν N-O), 1248 (ν C-N), 1178 (ν_s S=O), 752 (δ C_{sp2}-H), 672 (δ C_{sp2}-H) cm^{-1}. ^{1}H-NMR (400 MHz, DMSO-d_6): δ 3.32 (dd, ^2J = 17.2 Hz, ^3J = 6.8 Hz, 1H, C(4)H_2-isoxazoline), 3.56 (dd, ^2J = 17.2 Hz, ^3J = 10.4 Hz, 1H, C(4)H_2-isoxazoline), 3.79 (s, 3H, OCH_3), 3.85 (dd, ^2J = 15.2 Hz, ^3J = 4.8 Hz, 1H, CH_2), 3.97 (dd, ^2J = 15.2 Hz, ^3J = 7.6 Hz, 1H, CH_2), 5.02-5.10 (m, 1H, C(5)H-isoxazoline), 7.00 (d, ^3J = 8.8 Hz, 2H, Ar), 7.60 (d, ^3J = 8.8 Hz, 2H, Ar), 7.99-8.13 (m, 3H, Ar), 8.30 (d, ^3J = 7.6 Hz, 2H, Ar). ^{13}C-NMR (101 MHz, DMSO-d_6): δ 38.9 (C(4)H_2-isoxazoline), 42.5 (CH_2), 55.8 (OCH_3), 77.5 (C(5)H-isoxazoline), 114.7 (2 x Ar), 115.7 (Ar), 121.9 (Ar), 122.0 (Ar), 126.6 (Ar), 128.7 (2 x Ar), 135.8 (Ar), 136.2 (Ar), 137.1 (Ar), 157.0 (C=N, isoxazoline), 159.6 (Ar), 161.8 (C=O).

2-((3-Phenyl-4,5-dihydroisoxazol-5-yl)methyl)benzo[d]isothiazol-3(2H)-one 1,1-dioxide ***8a***. 2-Allylbenzo[*d*]isothiazol-3(*2H*)-one 1,1-dioxide **S1** (1 g, 0.0044 mol) and *N*-hydroxybenzimidoyl chloride **C8** (0.85 g, 0.0055 mol) were dissolved in 50 mL of anhydrous ethyl acetate. Triethylamine (0.76 mL, 0.0055 mol) in ethyl acetate was added dropwise over 30 min. A white suspension was formed and stirred overnight at room temperature. The reaction was quenched with 40 mL of water and the resulting suspension was extracted with dichloromethane (3 x 20 mL). The organics reunited were dried over sodium sulphate and evaporated *in vacuo.* Purification by column chromatography on silica gel (ethyl acetate:petroleum ether 1:3) gave the title compound as a thick oil (0.92 g, 60% yield); IR ν_{max} 2935 (ν C_{sp2}-H), 1729 (ν C=O), 1594 (ν C=N), 1331 (ν_{as} S=O), 1302 (ν N-O), 1256 (ν C-N), 1175 (ν_s S=O), 748 (δ C_{sp2}-H), 675 (δ C_{sp2}-H) cm^{-1}. ^{1}H-NMR (400 MHz, $CDCl_3$): δ 3.32-3.36 (m, 1H, C(4)H_2-isoxazoline), 3.42-3.49 (m, 1H, C(4)H_2-isoxazoline), 3.85-3.90 (m, 1H, CH_2), 4.01-4.05 (m, 1H, CH_2), 5.19 (br s, 1H, C(5)H-isoxazoline), 7.35 (br s, 3H, Ar), 7.64 (br s, 2H, Ar), 7.77-7.86 (m, 3H, Ar), 7.96-7.98 (m, 1H, Ar). ^{13}C-NMR (101 MHz, $CDCl_3$): δ 38.7

(C(4)H_2-isoxazoline), 41.8 (CH_2), 77.7 (C(5)H-isoxazoline), 121.1 (Ar), 125.3 (Ar), 126.9 (2 x Ar), 128.8 (2 x Ar), 129.1 (Ar), 130.3 (Ar), 134.6 (Ar), 135.3 (Ar), 137.3 (Ar), 156.6 (C=N, isoxazoline), 159.3 (C=O).

2-((3-(Thiophen-2-yl)-4,5-dihydroisoxazol-5-yl)methyl)benzo[d]isothiazol-3(2H)-one 1,1-dioxide ***9a***. 2-Allylbenzo[*d*]isothiazol-3(*2H*)-one 1,1-dioxide **S1** (1 g, 0.0044 mol) and *N*-hydroxythiophene-2-carbimidoyl chloride **C9** (0.89 g, 0.0055 mol) were dissolved in 50 mL of anhydrous ethyl acetate. Triethylamine (0.76 mL, 0.0055 mol) in ethyl acetate was added dropwise over 30 min. A white suspension was formed and stirred overnight at room temperature. The reaction was quenched with 40 mL of water and the resulting suspension was extracted with dichloromethane (3 x 20 mL). The organics reunited were dried over sodium sulphate and evaporated *in vacuo.* Purification by column chromatography on silica gel (ethyl acetate:*n*-hexane, 1:3) gave the title compound as a brown highly thick oil (1.16 g, 76% yield); IR ν_{max} 3091 (ν C_{sp2}-H), 1730 (ν C=O), 1636 (ν C=N), 1332 (ν_{as} S=O), 1311 (ν N-O), 1260 (ν C-N), 1178 (ν_s S=O), 752 (δ C_{sp2}-H), 698 (δ C_{sp2}-H) cm^{-1}. ^{1}H-NMR (400 MHz, $CDCl_3$): *δ* 3.38 (dd, ^2J = 16.4 Hz, ^3J = 6.4 Hz, 1H, C(4)H_2-isoxazoline), 3.51 (dd, ^2J = 16.8 Hz, ^3J = 10.4 Hz, 1H, C(4)H_2-isoxazoline), 3.90 (dd, ^2J = 14.8 Hz, ^3J = 7.2 Hz, 1H, CH_2), 4.05 (dd, ^2J = 14.8 Hz, ^3J = 5.6 Hz, 1H, CH_2), 5.18-5.22 (m, 1H, C(5)H-isoxazoline), 7.04-7.06 (m, 1H, thiophene), 7.04-7.06 (m, 1H, thiophene), 7.22-7.23 (m, 1H, thiophene), 7.39-7.40 (m, 1H, thiophene), 7.84-7.95 (m, 3H, Ar), 8.06 (d, J = 7.2 Hz, 1H, Ar). ^{13}C-NMR (101 MHz, $CDCl_3$): *δ* 39.6 (C(4)H_2-isoxazoline), 41.6 (CH_2), 77.8 (C(5)H-isoxazoline), 121.2 (Ar), 125.4 (thiophene), 126.9 (thiophene), 127.4 (Ar), 128.7 (thiophene), 129.0 (thiophene), 131.3 (Ar), 134.7 (Ar), 135.2 (Ar), 137.4 (Ar), 152.3 (C=N, isoxazoline), 159.3 (C=O).

Synthesis and characterization data for saccharin/isoxazole derivatives ***1b-9b***

2-((3-(3-Nitrophenyl)isoxazol-5-yl)methyl)benzo[d]isothiazol-3(2H)-one 1,1-dioxide ***1b***. 2-(Prop-2-yn-1-yl)benzo[*d*]isothiazol-3(2*H*)-one 1,1-dioxide **S2** (1 g, 0.0045 mol) and *N*-hydroxy-3-nitrobenzimidoyl chloride **C1** (1.12 g, 0.0056 mol) were dissolved in 50 mL of anhydrous ethyl acetate. Triethylamine (0.78 mL, 0.0056 mol) in ethyl acetate was added dropwise over 30 min. A

white suspension was formed and stirred overnight at room temperature. The reaction was quenched with 40 mL of water and the resulting suspension was extracted with dichloromethane (3 x 20 mL). The organics reunited were dried over sodium sulphate and evaporated *in vacuo*. Purification by column chromatography on silica gel (ethyl acetate:*n*-hexane 1:1) gave the title compound as a white solid (1.31 g, 76% yield); mp 191-193 °C; IR ν_{max} 1731 (ν C=O), 1605 (ν C=N), 1539 (ν_{as} N-O, NO_2), 1334 (ν_{as} S=O), 1303 (ν_s N-O, NO_2), 1262 (ν C-N), 1185 (ν_s S=O), 755 (δ C_{sp2}-H), 670 (δ C_{sp2}-H) cm^{-1}. ^{1}H-NMR (400 MHz, DMSO-d_6): δ 5.23 (s, 2H, CH_2), 7.37 (s, 1H, C(4)H, isoxazole), 7.79-7.81 (m, 1H, Ar), 8.02-8.10 (m, 2H, Ar), 8.15-8.17 (m, 1H, Ar), 8.31-8.33 (m, 2H, Ar), 8.35-8.37 (m, 1H, Ar), 8.61 (br s, 1H, Ar). ^{13}C-NMR (101 MHz, DMSO-d_6): δ 33.9 (CH_2), 102.7 (C(4)H-isoxazole), 121.6 (Ar), 122.3 (Ar), 125.4 (Ar), 125.9 (Ar), 126.6 (Ar), 130.2 (Ar), 131.4 (Ar), 133.4 (Ar), 135.9 (Ar), 136.6 (Ar), 137.3 (Ar), 148.8 (Ar), 158.7 (C(5)-isoxazole), 161.1 (C=N, isoxazole), 168.2 (C=O).

2-((3-(4-Nitrophenyl)isoxazol-5-yl)methyl)benzo[d]isothiazol-3(2H)-one 1,1-dioxide ***2b***. 2-(Prop-2-yn-1-yl)benzo[*d*]isothiazol-3(2*H*)-one 1,1-dioxide **S2** (1 g, 0.0045 mol) and *N*-hydroxy-4-nitrobenzimidoyl chloride **C2** (1.12 g, 0.0056 mol) were dissolved in 50 mL of anhydrous ethyl acetate. Triethylamine (0.78 mL, 0.0056 mol) in ethyl acetate was added dropwise over 30 min. A white suspension was formed and stirred overnight at room temperature. The reaction was quenched with 40 mL of water and the resulting suspension was filtered to give title compound as a white solid (1.14 g, 66% yield); mp 260-262 °C; IR ν_{max} 3145 (ν C_{sp2}-H), 1597 (ν C=N), 1720 (ν C=O), 1511 (ν_{as} N-O, NO_2), 1334 (ν_{as} S=O), 1303 (ν_s N-O), 1268 (ν C-N), 1184 (ν_s S=O), 755 (δ C_{sp2}-H), 677 (δ C_{sp2}-H) cm^{-1}. ^{1}H-NMR (400 MHz, DMSO-d_6): δ 5.23 (s, 2H, CH_2), 7.31 (s, 1H, C(4)H-isoxazole), 8.02-8.10 (m, 2H, Ar), 8.13-8.17 (m, 3H, Ar), 8.31-8.37 (m, 3H, Ar). ^{13}C-NMR (101 MHz, DMSO-d_6): δ 33.8 (CH_2), 102.9 (C(4)H-isoxazole), 122.3 (Ar), 124.8 (2 x Ar), 125.9 (Ar), 126.6 (Ar), 128.4 (2 x Ar), 134.6 (Ar), 135.9 (Ar), 136.6 (Ar), 137.3 (Ar), 148.9 (Ar), 155.2 (C=N, isoxazole), 158.7 (C(5)-isoxazole), 168.3 (C=O).

2-((3-(Pyridin-2-yl)isoxazol-5-yl)methyl)benzo[d]isothiazol-3(2H)-one 1,1-dioxide ***3b***. 2-(Prop-2-yn-1-yl)benzo[*d*]isothiazol-3(2*H*)-one 1,1-dioxide **S2** (1 g, 0.0045 mol) and *N*-hydroxy- pyridine-2-carbimidoyl chloride **C3** (0.87 g, 0.0056 mol) were dissolved in 50 mL of anhydrous ethyl acetate. Triethylamine (0.78 mL, 0.0056 mol) in ethyl acetate was added dropwise over 30 min. A white suspension was formed and stirred overnight at room temperature. The reaction was quenched with 40 mL of water and the resulting suspension was filtered to give title compound as a light brown solid (1.10 g, 72% yield); mp 161-164 °C; IR ν_{max} 3101 (ν C_{sp2}-H), 1735 (ν C=O), 1593 (ν C=N), 1326 (ν_{as} S=O), 1303 (ν N-O), 1269 (ν C-N), 1180 (ν_s S=O), 785 (δ C_{sp2}-H), 749 (δ C_{sp2}-H) cm^{-1}. ^{1}H-NMR (400 MHz, DMSO-d_6): δ 5.25 (s, 2H, CH_2), 7.06 (s, 1H, C(4)H-isoxazole), 7.48-7.50 (m, 1H, pyr), 7.92-8.08 (m, 2H Ar + 2H pyr), 8.14-8.16 (m, 1H, Ar), 8.35-8.37 (m, 1H, Ar), 8.68 (s, 1H, pyr). ^{13}C-NMR (101 MHz, DMSO-d_6): δ 33.8 (CH_2), 103.0 (C(4)H-isoxazole), 121.8 (pyr), 122.2 (Ar), 125.7 (Ar), 125.9 (pyr), 135.9 (Ar), 136.6 (Ar), 137.3 (Ar), 138.0 (Ar), 147.5 (pyr), 147.7 (pyr), 150.5 (pyr), 158.7 (C(5)-isoxazole), 163.5 (C=N, isoxazole), 167.7 (C=O).

2-((3-(Pyridin-3-yl)isoxazol-5-yl)methyl)benzo[d]isothiazol-3(2H)-one 1,1-dioxide ***4b***. 2-(Prop-2-yn-1-yl)benzo[*d*]isothiazol-3(2*H*)-one 1,1-dioxide **S2** (1 g, 0.0045 mol) and *N*-hydroxy- pyridine-3-carbimidoyl chloride **C4** (0.87 g, 0.0056 mol) were dissolved in 50 mL of anhydrous ethyl acetate. Triethylamine (0.78 mL, 0.0056 mol) in ethyl acetate was added dropwise over 30 min. A white suspension was formed and stirred overnight at room temperature. The reaction was quenched with 40 mL of water and the resulting suspension was extracted with dichloromethane (3 x 20 mL). The organics reunited were dried over sodium sulphate and evaporated *in vacuo.* Purification by column chromatography on silica gel (ethyl acetate:*n*-hexane, 1:1) gave the title compound as a light brown solid (0.98 g, 64% yield); mp 140-143 °C; IR ν_{max} 3084 (ν C_{sp2}-H), 1736 (ν C=O), 1610 (ν C=N), 1327 (ν_{as} S=O), 1292 (ν N-O), 1260 (ν C-N), 1173 (ν_s S=O), 747 (δ C_{sp2}-H), 671 (δ C_{sp2}-H) cm^{-1}. ^{1}H-NMR (400 MHz, $CDCl_3$): δ 5.11 (s, 2H, CH_2), 6.74 (s, 1H, C(4)H-isoxazole), 7.37-7.40 (m, 1H, pyr), 7.87-7.99 (m, 2H Ar + 1H pyr), 8.11-8.13 (d, J = 7.6 Hz, 2H, Ar), 8.67-8.68 (m, 1H, pyr), 8.98 (s, 1H, pyr). ^{13}C-NMR (101 MHz, $CDCl_3$): δ 33.6 (CH_2), 101.9 (C(4)H-isoxazole), 121.3 (Ar),

123.8 (pyr), 125.6 (Ar), 126.1 (pyr), 126.8 (Ar), 134.2 (pyr), 134.7 (Ar), 135.4 (Ar), 137.7 (Ar), 146.9 (pyr), 147.9 (pyr), 151.1 (C=N, isoxazole), 158.4 (C(5)-isoxazole), 166.6 (C=O).

2-((3-(2-Methoxyphenyl)isoxazol-5-yl)methyl)benzo[d]isothiazol-3(2H)-one 1,1-dioxide ***5b***. 2-(Prop-2-yn-1-yl)benzo[*d*]isothiazol-3(2*H*)-one 1,1-dioxide **S2** (1 g, 0.0045 mol) and *N*-hydroxy-2-methoxybenzimidoyl chloride **C5** (1.04 g, 0.0056 mol) were dissolved in 50 mL of anhydrous ethyl acetate. Triethylamine (0.78 mL, 0.0056 mol) in ethyl acetate was added dropwise over 30 min. A white suspension was formed and stirred overnight at room temperature. The reaction was quenched with 40 mL of water and the resulting suspension was extracted with dichloromethane (3 x 20 mL). The organics reunited were dried over sodium sulphate and evaporated *in vacuo*. Purification by column chromatography on silica gel (ethyl acetate:*n*-hexane, 1:1) gave the title compound as a white solid (1.45 g, 87% yield); mp 129-131 °C; IR ν_{max} 1733 (ν C=O), 1603 (ν C=N), 1337 (ν_{as} S=O), 1300 (ν N-O), 1250 (ν C-N), 1185 (ν_s S=O), 760 (δ C_{sp2}-H), 671 (δ C_{sp2}-H) cm^{-1}. ^{1}H-NMR (400 MHz, $CDCl_3$): *δ* 3.88 (s, 3H, OCH_3), 5.10 (s, 2H, CH_2), 6.93 (s, 1H, C(4)H-isoxazole), 6.97-7.04 (m, 2H, Ar), 7.39-7.42 (m, 1H, Ar), 7.86-7.91 (m, 3H, Ar), 7.94-7.96 (m, 1H, Ar), 8.08-8.10 (m, 1H, Ar). ^{13}C-NMR (101 MHz, $CDCl_3$): *δ* 33.6 (CH_2), 55.6 (OCH_3), 105.8 (C(4)H-isoxazole), 111.4 (Ar), 117.6 (Ar), 120.9 (Ar), 121.2 (Ar), 125.5 (Ar), 126.9 (Ar), 129.5 (Ar), 131.4 (Ar), 134.6 (Ar), 135.2 (Ar), 137.6 (Ar), 157.2 (Ar), 158.5 (C(5)-isoxazole), 160.4 (C=N, isoxazole), 164.3 (C=O).

2-((3-(3-Methoxyphenyl)isoxazol-5-yl)methyl)benzo[d]isothiazol-3(2H)-one 1,1-dioxide ***6b***. 2-(Prop-2-yn-1-yl)benzo[*d*]isothiazol-3(2*H*)-one 1,1-dioxide **S2** (1 g, 0.0045 mol) and *N*-hydroxy-3-methoxybenzimidoyl chloride **C6** (1.04 g, 0.0056 mol) were dissolved in 50 mL of anhydrous ethyl acetate. Triethylamine (0.78 mL, 0.0056 mol) in ethyl acetate was added dropwise over 30 min. A white suspension was formed and stirred overnight at room temperature. The reaction was quenched with 40 mL of water and the resulting suspension was extracted with dichloromethane (3 x 20 mL). The organics reunited were dried over sodium sulphate and evaporated *in vacuo*. Purification by column chromatography on silica gel (ethyl acetate:petroleum ether 1:3) gave the title compound as

a pale yellow solid (1.32 g, 79% yield); mp 147-149 °C; IR ν_{max} 2937 (ν C_{sp2}-H), 1740 (ν C=O), 1603 (ν C=N), 1328 (ν_{as} S=O), 1300 (ν N-O), 1255 (ν C-N), 1163 (ν_s S=O), 755 (δ C_{sp2}-H), 675 (δ C_{sp2}-H) cm^{-1}.^{1}H-NMR (400 MHz, DMSO-d_6): δ 3.80 (s, 3H, OCH_3), 5.22 (s, 2H, CH_2), 7.05-7.07 (m, 1H, Ar), 7.18 (s, 1H, C(4)H-isoxazole), 7.39-7.45 (m, 3H, Ar), 8.02 (t, J = 7.6 Hz, 1H, Ar), 8.07-8.11 (m, 1H, Ar), 8.16 (d, J = 7.6 Hz, 1H, Ar), 8.37 (d, J = 7.6 Hz, 1H, Ar). ^{13}C-NMR (101 MHz, DMSO-d_6): δ 33.8 (CH_2), 55.7 (OCH_3), 102.6 (C(4)H-isoxazole), 112.2 (Ar), 116.6 (Ar), 119.4 (Ar), 122.4 (Ar), 125.8 (Ar), 126.6 (Ar), 129.9 (Ar), 130.7 (Ar), 135.8 (Ar), 136.5 (Ar), 137.3 (Ar), 158.7 (C(5)-isoxazole), 160.1 (Ar), 162.5 (C=N, isoxazole), 167.3 (C=O).

2-((3-(4-Methoxyphenyl)isoxazol-5-yl)methyl)benzo[d]isothiazol-3(2H)-one 1,1-dioxide ***7b***. 2-(Prop-2-yn-1-yl)benzo[*d*]isothiazol-3(2*H*)-one 1,1-dioxide **S2** (1 g, 0.0045 mol) and *N*-hydroxy-4-methoxybenzimidoyl chloride **C7** (1.04 g, 0.0056 mol) were dissolved in 50 mL of anhydrous ethyl acetate. Triethylamine (0.78 mL, 0.0056 mol) in ethyl acetate was added dropwise over 30 min. A white suspension was formed, and the reaction stirred overnight at room temperature. The reaction was quenched with 40 mL of water and the resulting suspension was filtered to give the title compound as a white solid (1.48 g, 89% yield); mp 182-185 °C; IR ν_{max} 3127 (ν C_{sp2}-H), 1739 (ν C=O), 1614 (ν C=N), 1333 (ν_{as} S=O), 1294 (ν N-O), 1248 (ν C-N), 1169 (ν_s S=O), 834 (δ C_{sp2}-H), 752 (δ C_{sp2}-H) cm^{-1}; ^{1}H-NMR (400 MHz, DMSO-d_6): δ 3.80 (s, 3H, OCH_3), 5.18 (s, 2H, CH_2), 7.03-7.06 (m, 2H Ar + 1H C(4)H-isoxazole), 7.78-7.80 (m, 2H, Ar), 8.03-8.09 (m, 2H, Ar), 8.16-8.17 (m, 1H, Ar), 8.35-8.36 (m, 1H, Ar). ^{13}C-NMR (101 MHz, DMSO-d_6): δ 33.8 (CH_2), 55.7 (OCH_3), 102.1 (C(4)H-isoxazole), 115.0 (2 x Ar), 121.0 (Ar), 122.2 (Ar), 124.8 (Ar), 125.9 (Ar), 128.6 (2 x Ar), 135.9 (Ar), 136.6 (Ar), 137.2 (Ar), 156.0 (Ar), 158.7 (C(5)-isoxazole), 161.5 (C=N, isoxazole), 166.9 (C=O).

2-((3-Phenylisoxazol-5-yl)methyl)benzo[d]isothiazol-3(2H)-one 1,1-dioxide ***8b***. 2-(Prop-2-yn-1-yl)benzo[*d*]isothiazol-3(2*H*)-one 1,1-dioxide **S2** (1 g, 0.0045 mol) and *N*-hydroxybenzimidoyl chloride **C8** (0.87 g, 0.0056 mol) were dissolved in 50 mL of anhydrous ethyl acetate. Triethylamine (0.78 mL, 0.0056 mol) in ethyl acetate was added dropwise over 30 min. A white

suspension was formed and stirred overnight at room temperature. The reaction was quenched with 40 mL of water and the resulting suspension was extracted with dichloromethane (3 x 20 mL). The organics reunited were dried over sodium sulphate and evaporated *in vacuo.* Purification by column chromatography on silica gel (ethyl acetate:petroleum ether, 1:3) gave the title compound as a pale yellow solid (1.11 g, 73% yield); mp 127-130 °C; IR ν_{max} 3129 (ν C_{sp2}-H), 1741 (ν C=O), 1608 (ν C=N), 1333 (ν_{as} S=O), 1292 (ν N-O), 1256 (ν C-N), 1181 (ν_s S=O), 754 (δ C_{sp2}-H), 694 (δ C_{sp2}-H) cm^{-1}. ^{1}H-NMR (400 MHz, $CDCl_3$): δ 5.10 (s, 2H, CH_2), 6.71 (s, 1H, CH-isoxazole), 7.42-7.44 (m, 3H, Ar), 7.77-7.79 (m, 2H, Ar), 7.83-7.92 (m, 2H, Ar), 7.96 (d, ^{3}J = 7.2 Hz, 1H, Ar), 8.09 (d, ^{3}J = 7.6 Hz, 1H, Ar). ^{13}C-NMR (101 MHz, $CDCl_3$): δ 33.7 (CH_2), 102.2 (C(4)H-isoxazole), 121.3 (Ar), 125.6 (Ar), 126.8 (Ar), 126.9 (2 x Ar), 128.6 (Ar), 128.9 (2 x Ar), 130.2 (Ar), 134.7 (Ar), 135.3 (Ar), 137.6, 158.5 (C(5)-isoxazole), 162.7 (C=N, isoxazole), 165.9 (C=O).

2-((3-(Thiophen-2-yl)isoxazol-5-yl)methyl)benzo[d]isothiazol-3(2H)-one 1,1-dioxide ***9b***. 2-(Prop-2-yn-1-yl)benzo[*d*]isothiazol-3(2*H*)-one 1,1-dioxide **S2** (1 g, 0.0045 mol) and *N*-hydroxythiophene-2-carbimidoyl chloride **C9** (0.90 g, 0.0056 mol) were dissolved in 50 mL of anhydrous ethyl acetate. Triethylamine (0.78 mL, 0.0056 mol) in ethyl acetate were added dropwise over 30 min. A white suspension was formed and stirred overnight at room temperature. The reaction was quenched with 40 mL of water and the resulting suspension was extracted with dichloromethane (3 x 20 mL). The organics reunited were dried over sodium sulphate and evaporated *in vacuo.* Purification by column chromatography on silica gel (ethyl acetate:*n*-hexane, 1:3) gave the title compound as a white solid (1.20 g, 77% yield) mp 144-146 °C; IR ν_{max} 3136 (ν C_{sp2}-H), 1724 (ν C=O), 1612 (ν C=N), 1332 (ν_{as} S=O), 1300 (ν N-O), 1268 (ν C-N), 1175 (ν_s S=O), 752 (δ C_{sp2}-H), 706 (δ C_{sp2}-H) cm^{-1}. ^{1}H-NMR (400 MHz, $CDCl_3$): δ 5.09 (s, 2H, CH_2), 6.63 (s, 1H, C(4)H-isoxazole), 7.09-7.12 (m, 1H, thiophene), 7.42-7.46 (m, 2H, thiophene), 7.90-7.99 (m, 3H, Ar), 8.01-8.15 (m, 1H, Ar). ^{13}C-NMR (101 MHz, $CDCl_3$): δ 33.6 (CH_2), 102.2 (C(4)H, isoxazole), 121.3 (Ar), 125.6 (Ar), 126.8 (Ar), 127.6 (Ar, thiophene), 127.8 (Ar, thiophene), 127.9 (Ar, thiophene), 130.2 (Ar, thiophene), 134.7 (Ar), 135.3 (Ar), 137.6 (Ar), 157.9 (C=N, isoxazole), 158.5 (C(5)-isoxazole), 165.9 (C=O).

CA inhibition screening assay

An Applied Photophysics stopped-flow instrument has been used for assaying the CA-catalyzed CO_2 hydration activity. Phenol red, at a concentration of 0.2 mM, has been used as an indicator, working at the maximum absorbance of 557 nm with 20 mM Hepes, 4-(2-hydroxyethyl)-1-piperazineethanesulfonic acid, (pH 7.5 for α-CAs) as buffer and 20 mM Na_2SO_4 (for maintaining constant the ionic strength, but without inhibiting the enzyme). The initial rates of the CA-catalysed CO_2 hydration reaction were followed for a period of 10-100 s. The CO_2 concentrations ranged from 1.7 to 17 mM for the determination of the kinetic parameters and inhibition constants. For each inhibitor, at least six traces of the initial 5-10% of the reaction have been used for determining the initial velocity. The uncatalyzed rates were determined in the same manner and subtracted from the total observed ones. Stock solutions of each inhibitor (0.1 mM) were prepared in distilled−deionized water and dilutions up to 0.01 nM were done thereafter with distilled−deionized water. Inhibitor and enzyme solutions were preincubated together for 15 min at room temperature prior to assay to allow for the formation of the E-I complex. The inhibition constants were obtained by nonlinear least-squares methods using the Cheng-Prusoff equation and represent the mean from at least three different determinations. Errors were in the range of ± 5-10% of the reported K_I values. Human CA isoforms were recombinant enzymes obtained in-house as reported earlier.[33] The enzyme concentrations in the assay system were as follows: hCA I, 13.2 nM; hCA II, 8.4 nM; hCA IX, 7.9 nM; hCA XII, 15.2 nM.

HPLC enantioseparation

HPLC-grade ethanol was purchased from Sigma-Aldrich (Milan, Italy). HPLC enantioseparations were performed by using stainless-steel Chiralpak AS-H (250 mm x 4.6 mm, 5 μm and 250 mm x 10 mm, 5 μm) columns (Chiral Technologies Europe, Illkirch, France). The HPLC apparatus used for analytical enantioseparations consisted of a PerkinElmer (Norwalk, CT, USA) 200 LC pump equipped with a Rheodyne (Cotati, CA, USA) injector, a 50 μL sample loop, an HPLC PerkinElmer

oven and a PerkinElmer detector. The signal was acquired and processed by Clarity software (DataApex, Prague, Czech Republic).

In the analytical separations, fresh standard solutions of **8a** and **9a** were prepared shortly before by dissolving about 2 mg of analyte in 20 mL of ethanol. The injection volume was 20 μL. For semipreparative separation, a PerkinElmer 200 LC pump equipped with a Rheodyne injector, a 5000 μL sample loop, a PerkinElmer LC 101 oven and Waters 484 detector (Waters Corporation, Milford, MA, USA) were used. The feed solution for milligram enantioseparations was prepared by dissolving 50 mg of racemic samples in 10 mL of ethanol. The CD spectra (Figure 5, left and right) of the enantiomers collected on a semipreparative scale were recorded in ethanol at 25 °C by using a Jasco Model J-700 spectropolarimeter. The optical path was 0.1 mm. The spectra are average computed over three instrumental scans and the intensities are presented in terms of ellipticity values (mdeg).

Molecular modelling

Molecular Docking. The crystal structures of hCA I (PDB code 1AZM), hCA II (PDB code 2AW1), hCA IX (PDB code 3IAI) and hCA XII (PDB code 1JD0) were taken from the Protein Data Bank.[34] Molecular docking calculations were performed with GOLD 5.1[35] using GoldScore fitness function, as this procedure demonstrated to be particularly reliable in predicting the correct disposition of the zinc-binding groups of hCA ligands.[36] The region of interest for the docking studies was defined including all the residues which stayed within 10 Å from the bound ligand in the X-ray structures; the "allow early termination" option was deactivated, while the possibility for the ligand to flip ring corners was activated. The ligands were subjected to 30 genetic algorithm runs and all other settings were left as their defaults. The best docked conformation was taken into account for each ligand in each docking study.

Molecular dynamics simulations. Molecular dynamics (MD) simulations were performed with AMBER 16[37] using the ff14SB force field. Each ligand-protein complex was placed in a rectangular parallelepiped water box, using the TIP3P explicit solvent model for water, and solvated with a 15

Å water cap. Sodium ions were added as counter ions to neutralize the obtained systems. Prior to MD simulations, the systems were subjected to energy minimization in order to optimize the hCA-inhibitor complexes predicted by docking, as previously done.[38] Two minimization steps including 5000 cycles of steepest descent followed by conjugate gradient, until a convergence of 0.05 kcal/Å mol, were performed. In the first one, the protein was maintained rigid with a position restraint of 100 kcal/mol·Å^2, so that to minimize only the positions of the water molecules. In the second step, the whole system was energy minimized by applying a harmonic potential of 10 kcal/mol·Å^2 only to the protein α carbons. The minimized complexes were then used as the starting point for the MD simulations using a protocol derived from previous studies on hCA ligands.[39] A 0.5 ns constant-volume simulation, in which the temperature of the system was raised from 0 to 300 K, was initially performed. Subsequently, the system was subjected to 20 ns of constant-pressure simulation, keeping a constant temperature of 300 K with the use of Langevin thermostat. In both MD steps, the harmonic potential of 10 kcal/mol·Å^2 on the protein α carbons was maintained. All simulations were performed using particle mesh Ewald electrostatics with a cut-off of 10 Å for non-bonded interactions and periodic boundary conditions. A simulation step of 2.0 fs was employed, as all bonds involving hydrogen atoms were kept rigid using SHAKE algorithm, while General Amber force field (GAFF) parameters were used for the ligand, whose partial charges were calculated with the AM1-BCC method as implemented in the Antechamber suite of AMBER 16.

*Assignment of the absolute configuration to compounds **8a** and **9a**: simulation of the relevant ECD spectra*

The chiroptical properties of the enantiomers of compounds **8a** and **9a** were assessed by molecular modelling calculations. These were performed in two steps: *i*) extensive conformational search, concerning the structure of both **8a** and **9a**, followed by suitable selection of the energetically more representative conformations; ii) simulation of the Electronic Circular Dichroism relevant to the found, more populated, conformations of the species. The conformational search was based on a molecular mechanic approach (force field: MMFF), carried out by means of the systematic

algorithm implemented in the computer program SPARTAN 10 v.1.1.0 (Wavefunction Inc., 18401 Von Karman Avenue, Suite 370, Irvine, CA 92612, USA). Employed conditions in this analysis: all rotatable bonds were varied; 40 kJ × mol^{-1} as maximum energy gap from the lowest energy geometry imposed for kept conformations; $R^2 \geq 0.9$ the criterion adopted to define conformers as duplicates in the analysis of similarity between conformations.

*Compound **8a***. Starting from a geometry of (*S*) configuration of compound **8a**, the molecular mechanic conformational search afforded six different geometries which, afterword, were further optimized at the HF/3-21G* level of theory, also simulating the presence of ethanol as the solvent. Then, the only three conformations found within an energy range of 3 kcal/mol have again been subjected to structure optimization, performed this time at the higher level of theory B3LYP/6-31G*, again simulating the presence of ethanol as the solvent. Finally, the ECD spectra of such C_{1-3} conformers have been simulated through the algorithms implemented in the Amsterdam Density Functional (ADF) package v. 2007.01. The found final relative differences in energy of the conformers C_2 and C_3 with respect to the Global Minimum (GM) C_1 (0.00 kcal mol^{-1}) were: C_2= 0.40, C_3= 1.84 kcal mol^{-1}, at which correspond the following percentages of Boltzmann distribution: 64.3% (C_1), 32.8% (C_2) and 2.9% (C_3).

For each conformer the options set to perform the above quoted calculation were: optimization at the BLYP level of theory, employing the TZ2P large core basis set; ethanol as the solvent; 30 singlet and triplet excitations; diagonalization method: Davidson; velocity representation; scaling factor 0.85; peak width 25.0. The ECD profiles obtained for the C_1, C_2 and C_3 conformations were then weighted according to the pertinent Boltzmann distributions, and then merged to afford the final, overall, ECD spectrum related to the **(*S*)-8a** enantiomer.

The final simulated ECD spectrum, superimposed on the experimental ones relevant to the isolated enantiomers of **8a** have been reported in Figure 5. By inspection of the resulting plot, it can reasonably be inferred that to the first and second eluted enantiomers (green and red line in Figure 5, left side) of **8a** correspond to the (*R*) and (*S*) configurations, respectively.

*Compound **9a***. Starting from a geometry of (*S*) configuration of compound **9a**, the molecular mechanic conformational search afforded fifteen different geometries which, afterword, were further optimized, first at the HF/3-21G* level and then at the final B3LYP/6-31G* level of theory, also simulating the presence of ethanol as the solvent. Eight conformations were found within an energy range of 3 kcal/mol, seven of which characterized by very low Boltzmann populations (ranging from 6.7% to 2.2%), while the GM by a Boltzmann population of 62.4%. For such reason, only the GM was submitted to simulation of the ECD spectra by means of the ADF program. The options set to perform such calculation were: single point at the BLYP level of theory, employing the QZ4P large core basis set; ethanol as the solvent; 25 singlet excitations; diagonalization method: Davidson; velocity representation; scaling factor 0.91; peak width 35.0. The obtained ECD profile, superimposed on the experimental ones relevant to the isolated enantiomers of **9a**, has been reported in Figure 5, right side. By inspection of the resulting plot, it can reasonably be inferred that to the first and second eluted enantiomers (green and red line in the Figure 5) of **9a** correspond to the (*R*) and (*S*) configurations, respectively.

Pan Assay INterference compoundS (PAINS) evaluation

According to a recently published editorial,[40] all designed inhibitors have been analyzed by means of different theoretical tools such as ZINC PAINS Pattern Identifier,[41] False Positive Remover[42] and FAF-Drug4.[43] Our compounds were not reported as potential PAINS or covalent inhibitors by none of the considered algorithms.

MCF7 cell culture

MCF7 human breast adenocarcinoma cell line (ATCC® HTB-22™) was cultured in DMEM high glucose medium supplemented with 10% of foetal bovine serum (FBS), 1% of penicillin/streptomycin and 1% of l-glutamine (all purchased by EuroClone, Milan, Italy). Cell culture was maintained in an incubator in a humidified atmosphere with 5% CO_2 at 37 °C.

Phase contrast microscopy and MTT assay

MCF7 cells were seeded at cell density of 10000/well into a 96-well tissue culture plate and cultured for 24 h. After culture medium was removed and replaced by fresh medium supplemented with $CoCl_2$ 100 μM, as elsewhere already reported.[44] $CoCl_2$ pretreatment was maintained for 48 h to induce a hypoxic condition. Then, the metabolic activity of MCF7 was evaluated after 72 h of treatment with compounds **2b** and **7b** at doses ranging from 0.05 to 200 μM in combination with doxorubicin 2.5 μM on a 96-well polystyrene plate through MTT (3-(4,5-dimethylthiazol-2-yl)-2,5-diphenyltetrazolium bromide) assay (Sigma-Aldrich, Milan, Italy). Compounds were dissolved in DMSO with a final concentration of 0.2%.

Phase contrast images were acquired by means of a Leica DM 4000 light microscopy (Leica Cambridge Ltd., Cambridge, UK) equipped with a Leica DFC 320 camera (Leica Cambridge Ltd). After acquiring phase contrast images, MTT test was executed. MTT test is based on the capacity of viable cells to reduce MTT into a purple formazan salt. After 72 h of treatment, the medium was replaced by a new one containing 0.5 mg/mL of MTT and probed with cells for 5 h at 37 °C. The plate was incubated in DMSO solution for 30 min at 37 °C to solubilize salts and then read at 570 nm through a microplate reader (Multiskan GO, Thermo Scientific, MA, USA). Values obtained in the absence of cells were considered as background. Viability was normalized to control cells treated with DMSO 0.2%, $CoCl_2$ 100 μM and doxorubicin 2.5 μM.

Human Gingival Fibroblasts (HGFs) cell culture

A total of 10 healthy donors, subjected to the extraction of the third molar, signed the informed consent according to the Italian Legislation and with the code of Ethical Principles for Medical Research comprising Human Subjects of the World Medical Association (Declaration of Helsinki). The project obtained the approval of the Local Ethical Committee of the University of Chieti (Chieti, Italy; approval no. 1173, approved on 31/03/2016). Gingiva withdrawal and HGF culture was performed as already reported.[45]

LDH assay

HGF membrane integrity was assessed by measuring lactate dehydrogenase (LDH) leakage into the medium by means of a CytoTox 96 non-radioactive cytotoxicity assay (Promega Corporation, Madison, WI, USA). Released LDH in culture supernatants is measured with a 30-min coupled enzymatic assay, which results in the conversion of a tetrazolium salt (iodonitrotetrazolium violet) into a red formazan product.

HGFs were seeded into a 96-well tissue culture plate, cultured with DMEM high glucose medium, supplemented with 10% of FBS, 1% of penicillin/streptomycin (all purchased by EuroClone, Milan, Italy) and maintained at 37 °C in a humidified atmosphere of 5% (v/v) CO_2. After 24 h, cells were treated with compounds **2b** and **7b** at doses ranging from 0.05 to 200 μM up to 72 h. After the exposure times (24, 48 and 72 h), cell supernatants were harvested, centrifuged at 450 g for 4 min and stored on ice. The absorbance was measured at 490 and 690 nm with a spectrophotometer (Multiskan GO, Thermo Scientific, Monza, Italy). The results were expressed according to the formula: %LDH released=[(A-B)/(C-B)*100, with A=LDH activity measured at 490 nm, B=LDH activity measured at 690 nm (background) and C=LDH activity of the positive control (cell lysate).

MTT assay

HGFs were seeded, cultured and treated with compounds **2b** and **7b**, as previously described for LDH assay. Compounds were dissolved in DMSO with a final vehicle concentration of 0.2%. HGFs viability was evaluated after 24, 48 and 72 h of treatment by means of MTT test following the procedure mentioned above. Viability was normalized to control cells treated with DMSO 0.2%.[46]

Statistics

Statistical analysis was executed with GraphPad 7 software using Ordinary One-Way ANOVA followed by post-hoc Tukey's multiple comparisons tests. Values of $p < 0.05$ were considered statistically significant.

Associated Content

Supporting Information

Additional figures illustrating molecular modelling data, the chromatographic profile for purity assessment, and *in vitro* cell-based assays. SMILES representation for compounds was reported as CSV file. This material is available free of charge on the ACS Publications website at DOI:

AUTHOR INFORMATION

Corresponding Author

*Phone: (0039) 06 49913975. E-mail: daniela.secci@uniroma1.it

Notes

The authors declare no competing financial interest.

ABBREVIATION USED

h, human; CA, carbonic anhydrase; MD, molecular dynamics; NCS, *N*-chlorosuccinimide; DMF, *N*,*N*-dimethylformamide; FBS, foetal bovine serum; FMO, frontier molecular orbitals; 2D, two dimensional; HGF, human gingival fibroblasts; LDH, lactate dehydrogenase; MTT, 3-(4,5-dimethylthiazol-2-yl)-2,5-diphenyltetrazolium bromide; NOESY, Nuclear Overhauser Effect Spectroscopy; HPLC; high-performance liquid chromatography; K_I, inhibition constant; ECD, electronic circular dichroism; i.d., internal diameter; mp, melting point; AAZ, acetazolamide; PBD, Protein Data Bank; $CDCl_3$, deuterated chloroform; DMSO, dimethyl sulphoxide; CD_3OD, deuterated methanol; CD_3CN, deuterated acetonitrile; br, broad; s, singlet; d, doublet; t, triplet; q, quartet; m, multiplet; Hepes, 4-(2-hydroxyethyl)-1-piperazineethanesulfonic acid; GAFF, General Amber Force Field; MMFF, molecular mechanic force field; ADF, Amsterdam Density Functional; GM, Global Minimum.

References

(1) Supuran, C. T. Structure and function of carbonic anhydrases. *Biochem. J.* **2016**, *473*, 2023-2032.

(2) Supuran, C. T. Carbonic anhydrases: novel therapeutic applications for inhibitors and activators. *Nat. Rev. Drug Discov.* **2008**, *7*, 168-181.

(3) Neri, D.; Supuran, C. T. Interfering with pH regulation in tumours as a therapeutic strategy. *Nat. Rev. Drug Discov.* **2011**, *10*, 767-77.

(4) Supuran, C. T. Carbonic anhydrase inhibitors as emerging agents for the treatment and imaging of hypoxic tumors. *Expert Opin. Investig. Drugs.* **2018**, *27*, 963-970.

(5) Supuran, C. T.; Alterio, V.; Di Fiore, A.; D'Ambrosio, K.; Carta, F.; Monti, S.M.; De Simone, G. Inhibition of carbonic anhydrase IX targets primary tumors, metastases, and cancer stem cells: Three for the price of one. *Med. Res. Rev.* **2018**, *38*, 1799-1836.

(6) Vullo, D.; Durante, M.; Di Leva, F.S.; Cosconati, S.; Masini, E.; Scozzafava, A.; Novellino, E.; Supuran, C. T.; Carta, F. Monothiocarbamates strongly inhibit carbonic anhydrases in vitro and possess intraocular pressure lowering activity in an animal model of glaucoma. *J. Med. Chem.* **2016**, *59*, 5857-5867.

(7) Carta, F.; Aggarwal, M.; Maresca, A.; Scozzafava, A.; McKenna, R.; Masini, E.; Supuran, C. T. Dithiocarbamates strongly inhibit carbonic anhydrases and show antiglaucoma action in vivo. *J. Med. Chem.* **2012**, *55*, 1721-1730.

(8) Alterio, V.; Di Fiore, A.; D'Ambrosio, K.; Supuran, C. T.; De Simone, G. Multiple binding modes of inhibitors to carbonic anhydrases: how to design specific drugs targeting 15 different isoforms? *Chem. Rev.* **2012**, *112*, 4421-4468.

(9) D'Ascenzio, M.; Carradori, S.; Secci, D.; Vullo, D.; Ceruso, M.; Akdemir, A.; Supuran, C. T. Selective inhibition of human carbonic anhydrases by novel amide derivatives of probenecid: synthesis, biological evaluation and molecular modelling studies. *Bioorg. Med. Chem.* **2014**, *22*, 3982-3988.

(10) D'Ambrosio, K.; Carradori, S.; Monti, S. M.; Buonanno, M.; Secci, D.; Vullo, D.; Supuran, C. T.; De Simone, G. Out of the active site binding pocket for carbonic anhydrase inhibitors. *Chem. Commun. (Camb).* **2015**, *51*, 302-305.

(11) Carradori, S. Selective carbonic anhydrase IX inhibitors based on coumarin scaffold as promising antimetastatic agents: WO2012070024. *Expert Opin. Ther. Pat.* **2013**, *23*, 751-756.

(12) Ivanova, J.; Carta, F.; Vullo, D.; Leitans, J.; Kazaks, A.; Tars, K.; Žalubovskis, R.; Supuran, C. T. *N*-Substituted and ring opened saccharin derivatives selectively inhibit transmembrane, tumor-associated carbonic anhydrases IX and XII. *Bioorg. Med. Chem.* **2017**, *25*, 1–7.

(13) D'Ascenzio, M.; Guglielmi, P.; Carradori, S.; Secci, D.; Florio, R.; Mollica, A.; Ceruso, M.; Akdemir, A.; Sobolev, A. P.; Supuran, C. T. Open saccharin-based secondary sulfonamides as potent and selective inhibitors of cancer-related carbonic anhydrase IX and XII isoforms. *J. Enzyme Inhib. Med. Chem.* **2017**, *32*, 51–59.

(14) Carradori, S.; Secci, D.; De Monte, C.; Mollica, A.; Ceruso, M.; Akdemir, A.; Sobolev, A. P.; Codispoti, R.; De Cosmi, F.; Guglielmi, P.; Supuran, C. T. A novel library of saccharin and acesulfame derivatives as potent and selective inhibitors of carbonic anhydrase IX and XII isoforms. *Bioorg. Med. Chem.* **2016**, *24*, 22–25.

(15) Coviello, V.; Marchi, B.; Sartini, S.; Quattrini, L.; Marini, A. M.; Simorini, F.; Taliani, S.; Salerno, S.; Orlandi, P.; Fioravanti, A.; Desidero, T.D.; Vullo, D.; Da Settimo, F.; Supuran, C. T.; Bocci, G.; La Motta, C. 1,2-Benzisothiazole derivatives bearing 4-, 5-, or 6-alkyl/arylcarboxamide moieties inhibit carbonic anhydrase isoform IX (CAIX) and cell proliferation under hypoxic conditions. *J. Med. Chem.* **2016**, *59*, 6547–6552.

(16) Alterio, V.; Tanc, M.; Ivanova, J.; Zalubovskis, R.; Vozny, I.; Monti, S. M.; Di Fiore, A.; De Simone, G.; Supuran, C. T. X-ray crystallographic and kinetic investigations of 6-sulfamoyl-saccharin as a carbonic anhydrase inhibitor. *Org. Biomol. Chem.* **2015**, *13*, 4064–4069.

(17) D'Ascenzio, M.; Carradori, S.; De Monte, C.; Secci, D.; Ceruso, M.; Supuran, C. T. Design, synthesis and evaluation of *N*-substituted saccharin derivatives as selective

inhibitors of tumor-associated carbonic anhydrase XII. *Bioorg. Med. Chem.* **2014**, *22*, 1821–1831.

(18) Moeker, J.; Peat, T. S.; Bornaghi, L. F.; Vullo, D.; Supuran, C. T.; Poulsen, S. A. Cyclic secondary sulfonamides: Unusually good inhibitors of cancer-related carbonic anhydrase enzymes. *J. Med. Chem.* **2014**, *57*, 3522–3531.

(19) Ivanova, J.; Carta, F.; Vullo, D.; Leitans, J.; Kazaks, A.; Tars, K.; Žalubovskis, R.; Supuran, C. T. *N*-Substituted and ring opened saccharin derivatives selectively inhibit transmembrane, tumor-associated carbonic anhydrases IX and XII. *Bioorg. Med. Chem.* **2017**, *25*, 3583–3589.

(20) Gothelf, K. V; Jørgensen, K. A. Asymmetric 1,3-dipolar cycloaddition reactions. *Chem. Rev.* **1998**, *98*, 863–909.

(21) Mabrour, M.; Bougrin, K.; Benhida, R.; Loupy, A.; Soufiaoui, M. An efficient one-step regiospecific synthesis of novel isoxazolines and isoxazoles of *N*-substituted saccharin derivatives through solvent-free microwave-assisted [3+2] cycloaddition. *Tetrahedron Lett.* **2007**, *48*, 443–447.

(22) Liu, K. C.; Shelton, B. R.; Howe, R. K. Particularly convenient preparation of benzohydroximinoyl chlorides (nitrile oxide precursors). *J. Org. Chem.* **1980**, *45*, 3916–3918.

(23) Huisgen, R. 1,3-Dipolar cycloadditions. 76. Concerted nature of 1,3-dipolar cycloadditions and the question of diradical intermediates. *J. Org. Chem.* **1976**, *41*, 403-419.

(24) Khalifah, R. G. The carbon dioxide hydration activity of carbonic anhydrase. I. Stop flow kinetic studies on the native human isoenzymes B and C. *J. Biol. Chem.* **1971**, *246*, 2561-2573.

(25) Simstein, R.; Burow, M.; Parker, A.; Weldon, C.; Beckman, B. Apoptosis, chemoresistance, and breast cancer: insights from the MCF-7 cell model system. *Exp. Biol. Med. (Maywood)* **2003**, *228*, 995-1003.

(26) Patil, V. V.; Gayakwad, E. M.; Shankarling, G. S. Highly efficient and stable peracid for rapid and selective oxidation of aliphatic amines to oximes. *New J. Chem.* **2015**, *39*, 6677–6682.

(27) Yu, J.; Lu, M. Metal-Free: A novel and efficient aerobic oxidation of primary amines to oximes using *N*,*N*',*N*''-trihydroxyisocyanuric acid and acetaldoxime as catalysts in water. *Synlett* **2014**, *25*, 1873–1878.

(28) Yano, J. K.; Denton, T. T.; Cerny, M. A.; Zhang, X.; Johnson, E. F.; Cashman, J. R. Synthetic inhibitors of cytochrome P-450 2A6: Inhibitory activity, difference spectra, mechanism of inhibition, and protein cocrystallization. *J. Med. Chem.* **2006**, *49*, 6987–7001.

(29) Tselinskii, I. V; Romanova, T. V Synthesis and reactivity of carbohydroximoyl azides: I. Aliphatic and aromatic carbohydroximoyl azides and 5-substituted 1-hydroxytetrazoles based thereon. *Russ. J. Org. Chem.* **2001**, *37*, 1638–1642.

(30) Demina, O. V.; Khodonov, A. A.; Sinauridze, E. I.; Shvets, V. I.; Varfolomeev, S. D. 5-Substituted pyridylisoxazoles as effective inhibitors of platelet aggregation. *Russ. Chem. Bull.* **2014**, *63*, 2092–2113.

(31) Dubrovskiy, A.; Larock, R. Synthesis of benzisoxazoles by the cycloaddition of in situ generated nitrile oxides and arynes. *Org. Lett.* **2010**, *12*, 1180–1183.

(32) Sanders, B. C.; Friscourt, F.; Ledin, P. A.; Mbua, N. E.; Arumugam, S.; Guo, J.; Boltje, T. J.; Popik, V. V.; Boons, G. J. Metal-free sequential [3 + 2]-dipolar cycloadditions using cyclooctynes and 1,3-dipoles of different reactivity. *J. Am. Chem. Soc.* **2011**, *133*, 949–957.

(33) Carradori, S.; De Monte, C.; D'Ascenzio, M.; Secci, D.; Celik, G.; Ceruso, M.; Vullo, D.; Scozzafava, A.; Supuran; C. T. Salen and tetrahydrosalen derivatives act as effective inhibitors of the tumor-associated carbonic anhydrase XII - A new scaffold for designing isoform-selective inhibitors. *Bioorg. Med. Chem. Lett.* **2013**, *23*, 6759-6763.

(34) Berman, H. M.; Westbrook, J.; Feng, Z.; Gilliland, G.; Bhat, T. N.; Weissig, H.; Shindyalov, I. N.; Bourne, P. E. The Protein Data Bank. *Nucleic Acids Res.* **2000**, *28*, 235-242.

(35) Verdonk, M. L.; Cole, J. C.; Hartshorn, M. J.; Murray, C. W.; Taylor, R. D. Improved protein-ligand docking using GOLD. *Proteins* **2013**, *52*, 609–623.

(36) Tuccinardi, T.; Nuti, E.; Ortore, G.; Supuran, C. T.; Rossello, A.; Martinelli, A. Analysis of human carbonic anhydrase II: docking reliability and receptor-based 3D-QSAR study. *J. Chem. Inf. Model.* **2007**, *47*, 515-525.

(37) Case, D. A.; Betz, R. M.; Cerutti, D. S.; Cheatham, T. E., III; Darden, T. A.; Duke, R. E.; Giese, T. J.; Gohlke, H.; Goetz, A. W.; Homeyer, N.; Izadi, S.; Janowski, P.; Kaus, J.; Kovalenko, A.; Lee, T. S.; LeGrand, S.; Li, P.; Lin, C.; Luchko, T.; Luo, R.; Madej, B.; Mermelstein, D.; Merz, K. M.; Monard, G.; Nguyen, H.; Omelyan, I.; Onufriev, A.; Roe, D. R.; Roitberg, A.; Sague, C.; Simmerling, C. L.; Botello-Smith, W. M.; Swails, J.; Walker, R. C.; Wang, J.; Wolf, R. M.; Wu, X.; Xiao, L.; Kollman, P. A. AMBER, version 16; University of California: San Francisco, CA, 2016.

(38) Krasavin, M.; Shetnev, A.; Sharonova, T.; Baykov, S.; Kalinin, S.; Nocentini, A.; Sharoyko, V.; Poli, G.; Tuccinardi, T.; Presnukhina, S.; Tennikova, T. B.; Supuran, C. T. Continued exploration of 1,2,4-oxadiazole periphery for carbonic anhydrase-targeting primary arene sulfonamides: Discovery of subnanomolar inhibitors of membrane-bound hCA IX isoform that selectively kill cancer cells in hypoxic environment. *Eur. J. Med. Chem.* **2019**, *164*, 92-105.

(39) Buran, K.; Bua, S.; Poli, G.; Önen Bayram, F. E.; Tuccinardi, T.; Supuran, C. T. Novel 8-substituted coumarins that selectively inhibit human carbonic anhydrase IX and XII. *Int. J. Mol. Sci.* **2019**, *20*, pii: E1208.

(40) Aldrich, C.; Bertozzi, C.; Georg, G. I.; Kiessling, L.; Lindsley, C.; Liotta, D.; Merz Jr., K. M.; Schepartz, A.; Wang, S. *J. Med. Chem.* **2017**, *60*, 2165-2168.

(41) http://zinc15.docking.org/patterns/home (accessed Aug 25 2019).

(42) Baell, J. B.; Holloway, G. A. New substructure filters for removal of pan assay interference compounds (PAINS) from screening libraries and for their exclusion in bioassays. *J. Med. Chem.* **2010**, *53*, 2719-2740. http://www.cbligand.org/PAINS (accessed Aug 25 2019).

(43) Lagorce, D.; Sperandio, O.; Galons, H.; Miteva, M. A.; Villoutreix, B. O. FAF-Drugs2: free ADME/tox filtering tool to assist drug discovery and chemical biology projects. *BMC Bioinformatics* **2008**, *9*, 396-405. http://fafdrugs3.mti.univ-paris-diderot.fr (accessed Aug 25 2019).

(44) Wu, D.; Yotnda, P. Induction and testing of hypoxia in cell culture. *J. Vis. Exp.* **2011**, *12*, pii: 2899.

(45) De Colli, M.; Tortorella, P.; Marconi, G.D.; Agamennone, M., Campestre, C.; Tauro, M.; Cataldi, A.; Zara, S. In vitro comparison of new bisphosphonic acids and zoledronate effects on human gingival fibroblasts viability, inflammation and matrix turnover. *Clin. Oral Invest.* **2016**, *20*, 2013-2021.

(46) Marconi, G.D.; Gallorini, M.; Carradori, S.; Guglielmi, P.; Cataldi, A.; Zara, S. The up-regulation of oxidative stress as a potential mechanism of novel MAO-B inhibitors for glioblastoma treatment. *Molecules* **2019**, *24*, 2005; doi:10.3390/molecules24102005.

Table of Contents graphic